IMPORTANT CONSIDERATIONS AND EXPERIMENTAL PROCEDURES FOR PROPERTIES MEASUREMENTS AND INTERNAL IMAGING BY MODERN ULTRASONIC METHODS*

Mahesh C. Bhardwaj
ULTRAN LABORATORIES, INC.
State College, PA 16801

TABLE OF CONTENTS

*Submitted to the Ceramic Bulletin, the American Ceramic Society
October 1988

IMPORTANT CONSIDERATIONS AND EXPERIMENTAL PROCEDURES FOR PROPERTIES MEASUREMENT AND INTERNAL IMAGING BY MODERN ULTRASONIC METHODS*

Mahesh C. Bhardwaj+
Ultran Laboratories, Inc.
State College, PA

INTRODUCTION

During the last two decades we have been witnessing the rapid development of structural materials necessitated by the space programs of the United States, U.S.S.R, and Europe. Supplemented by sophisticated advancements in electronics, this revolution has touched every walk of modern life. What was originally conceived for the aircraft and aerospace industries has come into the modern household through better construction materials, kitchen equipment, telecommunication, advanced automobiles, and even sporting and leisure goods! In the medical field, modern materials are continuously opening doors for "bionic" type replacements in the human body. Applications, development, and manufacture of new materials have advanced the industry by leaps and bounds. Everyone is benefitting from the materials revolution.

However, in trying to understand materials during their stages of development, manufacture, and applications, fewer technologies have attracted the attention of the materials community than the ones related to NonDestructive Characterization (NDC).

As the hunger for super-strength, super-light weight, *environmentally-insensitive, and cost-effective* materials continues, the need for reliable nondestructive analysis is becoming serious and unavoidable. Consider, for example the role of materials in the global thrust of *super-aeroplanes, super-automobiles, super-speed railroads, and mega-highways.* These industries together use thousands of materials (converted into millions of components) performing multiple mechanical and electronic functions under the most extreme chemical and physical environments. Indeed, it would be most desirable to know the condition and characteristics of a material or its component before it is applied to its intended use!

Whether one is concerned with economy, safety, or both, the role of nondestructive evaluation of materials cannot be overestimated. This paper deals with the development of scientifically viable and usable NDC methods using ultrasound as the characterizing tool. By utilizing laboratory-made and real world materials - ceramics, polymers, metals, and their composites - we will show advanced, and in some cases, even new methods of NDC and their applications at all levels of material manufacture and applications.

A perspective on ultrasonic NDC of materials and processes is shown in Fig. 1 and the principles of ultrasound for materials characterization is summarized in Fig. 2. The crux of ultrasonic methods is analogous to any other materials characterization technique that also utilizes some wave as an analytical tool. Measurement of ultrasonic/acoustic parameters of a test material, and their correlation with the properties of that material, is the foundation of NDC, Bhardwaj (1986),[1] Vary (1987).[2]

*Several portions of this paper were presented at the 89th and 90th annual meetings of the American Ceramic Society.
+Member American Ceramic Society

1. ULTRASONIC NDC FOR MATERIAL PROPERTY DETERMINATION

It should be noted that the subject of ultrasonic characterization is not new. It has been known for nearly 100 years, and has been in use as NonDestructive Testing (NDT), primarily in the metals industries. The major goal of NDT is to identify and locate "overt" flaws in metals. On the other hand, correlations of acoustic measurements (ultrasonic velocities, frequency dependence of ultrasound attenuation, and phase relations of reflected and transmitted ultrasonic signals) with test material properties (density, porosity, inter-granular or inter-crystalline relationships, elastic and mechanical properties) establish the basis for NonDestructive Characterization (NDC). In an attempt to exhibit the reliability of ultrasound for meaningful NDC, Vary (1987)[2], Thompson (1982-88)[3], Bhardwaj (1987)[4], and others have demonstrated advancements in time and frequency domain analysis of a wide range of industrial materials. While the advantages of nondestructive evaluation are numerous and evident, it should be noted that NDC is a relatively new subject. Ultrasonic methods and experimental techniques for further properties and micro-structure characterization need to be further developed.

In the succeeding sections we show systematic characterization of model ceramic and polymer materials in time domain by applying *material-suitable acoustics* and *material-suitable methodologies* developed at Ultran Laboratories.

1.1 Experimental Techniques

In order to determine the velocities of ultrasound in test materials, pulsed ultrasound (Fig. 3) was used to measure Times-Of-Flight (TOF) by the direct transmission method. Excitation of transducers and amplification of transmitted signals were performed by Ultran HF 400 system, featuring 5ns pulser rise time and a 35MHz amplifier bandwidth. When the test materials were extraordinarily porous, this system was replaced by Ultran HE 900, featuring tunable -ve spike 900 volt rf pulser and 3MHz amplifier bandwidth. Measurements of TOF corresponding to the known distance traveled by ultrasound were made from a Tektronix 2432, a 300MHz digitizing storage oscilloscope.
TOFs were measured by first establishing a reference signal corresponding to the "zero" position on the oscilloscope, as shown in Fig. 4. Fig. 4a shows the time domain trace of the triggered oscilloscope, i.e., without connecting cables and transducers. In order to establish the "zero" reference point it is important that TOF corresponding to the transducer matching/protective layers be taken account, otherwise they would introduce an error in test sample TOF. This is shown in Fig. 4b. Here, the two transducers - transmitter and receiver - were placed together with their active regions touching each other. The ensuing transmitted signal in this case corresponds to the TOF through the matching/protective layers of two transducers. At the trailing edge of this signal was placed a cursor , indicating the zero or the reference point from where TOFs corresponding to test sample travel distance were measured. For example, Fig. 4c shows the appearance of a transmitted signal through a test sample. The right hand cursor of Fig. 4c is placed at the trailing edge of the transmitted signal. The difference between the two cursors is the true TOF of ultrasound through the test sample, and is directly displayed on the oscilloscope screen.

Other methods, such as direct reflection or delayed reflection, may also be utilized for the measurement of TOF. However, such methods may exhibit limitations, particularly while studying relatively porous media. A technique utilizing this method for accurate TOF measurement is the "pulse-echo overlap," described by Vary (1980)[5]. It should be noted that this technique is only applicable to those ultrasonic signals that are

generated by direct reflection and feature multiple reflections, generally corresponding to the far side of a test sample. However, a wide range of industrial materials (super-dense to super-porous, chemically and physically heterogeneous, etc.) cannot be analyzed for accurate TOF measurements by pulse-echo overlap. This is due to frequency attenuation and other factors, which are likely to curb the usage of direct reflection method, a pre-requisite for "pulse-echo overlap." Furthermore, for extreme accuracy in TOF measurements, it is highly desirable to work within a well-collimated beam of ultrasound. This requirement can be satisfied more easily by using the direct transmission method. Pulse echo overlap technique, particularly on relatively thick material sections is also liable to introduce unwanted ultrasonic diffraction effects, thus adversely affecting the TOF measurements. For materials characterization, a more universal method for accurate TOF measurement is the direct transmission of ultrasound through the medium of propagation. However, if for some practical reasons, this method cannot be used, then other methods need to be applied.

1.2 Characterization of sintered Alumina

In order to exhibit time domain velocity relationships, various samples of sintered alumina (prepared at the Ceramic Science Section, Penn State University) - 51mm diameter and 13mm thick - were studied by the experimental procedure described in section 1.1. Microstructurally, these samples are characterized by open porosity, varying from 0.7% to 35.2% (theoretical density from 99.3% to 64.8%). Therefore, they were analyzed by "Dry Coupling" ultrasonic transducers, developed at Ultran. Significance of Dry Coupling over the conventional "Wet Coupling" has been described in details by Bhardwaj (1987).[4] Table I shows the salient characteristics of longitudinal and zero degree incident beam shear wave dry coupling transducers used in this investigation.

Fig. 5 shows a graphical relationship between the velocities of longitudinal and shear waves as functions of the density of sintered alumina. In order to establish the accuracy of velocity measurement, all samples were investigated as functions of varying frequencies of longitudinal and shear waves. Results of this study are shown in Fig. 6. It is observed that while longitudinal wave velocity can be measured within reasonable degree of accuracy between 5 to 20MHz frequencies, the same isn't true for shear wave velocities. The fact that lower shear wave frequencies - <5MHz - consistently generated lower velocities indicates one or two

ALUMINA DENSITY RANGE	DRY COUPLING TRANSDUCERS			
	LONGITUDINAL WAVE		SHEAR WAVE	
	Active Φ (mm)	Frequency (MHz)	Active Φ (mm)	Frequency (MHz)
99.3 - 92.3%	3.0	20.0	6.0	10.0
87.2 - 77.3%	6.0	10.0	6.0	5.0
70.3 - 64.8	12.7	5.0	12.7	2.0
"	12.7	2.0	12.7	1.0

Table I. Salient characteristics of Dry Coupling Longitudinal and Shear wave Transducers used for the NDC of alumina varying in density.

reasons: either the accuracy of shear wave measurement is reduced at lower frequencies, or shear waves react preferentially as a function of frequency. Before

arriving at specific conclusions, this phenomenon is being further evaluated, Bhardwaj (1988).[6]

Longitudinal and shear wave velocities are directly related to the elastic properties of the travel medium as follows:

$$E = V_l^2 \cdot \rho \cdot (1+\sigma) \cdot (1-2\sigma)/(1-\sigma) \quad (1)$$

$$G = V_t^2 \cdot \rho \quad (2)$$

$$\sigma = 1 - 2b^2/2-2b^2 \text{ , where} \quad (3)$$

$$b = V_t/V_l$$

$$K = E/3(1-2\sigma) \quad (4)$$

E = Young's modulus, GPa
G = Shear modulus, GPa
K = Bulk modulus, GPa
ρ = Density, g/cc
σ = Poisson's Ratio

By utilizing these relations in conjunction with measured longitudinal and shear wave velocities, Young and shear moduli of elasticity of sintered alumina were determined. These results are shown in Fig. 7. Fig. 8 is the comparison of destructively (static 4-point bending method) and nondestructively (as per the procedures described here) determined Young's modulus of elasticity of sintered alumina. The comparison of ultrasonically measured elastic modulus with that of conventional destructive method is excellent. It should be noted that since ultrasonic method is dynamic, the values of elastic modulus so obtained are generally higher than those from static methods. Table II shows acoustic and elastic properties of sintered alumina determined by ultrasonic dry coupling nondestructive methods.

1.3 Characterization of green stage ceramics

Correlation of ultrasonic velocities with compaction pressures or densities of green stage ceramics can also provide significant information, prior to their sintering. Before the successful development of dry coupling transducers, green or fragile materials could not be evaluated in a reliable manner. It is a matter of common sense that the conventional wet coupling of materials at such stages is likely to destroy and alter their original characteristics. However, this limitation has been effectively eliminated by the advent of dry coupling ultrasonics from our laboratory, Bhardwaj (1987).[4]

In order to demonstrate the applicability of modern ultrasonic NDC for green stage ceramics evaluation, several samples of compacted alumina-polymer binder (prepared at the Ceramic Science Section, Penn State University) were analyzed by the procedure described in section 1.1. These samples are typically 38mm diameter and 13mm thick and prepared at various compaction pressures. The dry coupling longitudinal and shear wave transducers are

12.7mm active area diameter and 1.0MHz nominal frequency. Results of this analysis are shown in Fig. 9.

ALUMINA DENSITY g/cc (% Theo.)	Vl (m/s)	Vt (m/s)	Z (10^5g/cm^2.s)[a]	E (GPa)	G (GPa)	K (GPa)	POISSON'S RATIO
3.98 (100)*	11,055	6,700	44.00	432	178	248	0.210
3.96 (99.3)	10,830	6,270	42.88	388	156	255	0.247
3.81 (95.6)	10,340	6,115	39.4	351	142	216	0.230
3.68 (92.3)	9,915	5,815	36.48	308	142	195	0.237
3.48 (87.2)	9,470	5,700	32.95	272	111	161	0.222
3.37 (84.5)	9,130	5,660	30.77	258	109	134	0.181
3.08 (77.3)	8,280	5,190	25.50	195	83	101	0.177
2.80 (70.3)	7,140	4,500	20.00	133	57	67	0.170
2.58 (64.8)	5,930	3,700	15.30	85	36	41	0.164

*Sapphire

[a]Acoustic impedance - product of longitudinal wave velocity and density.

Table II. Acoustic and elastic properties of alumina determined by ultrasonic dry coupling nondestructive methods.

1.4 Characterization of ultra porous ceramics

Materials, such as *rigid porous ceramics,* composed of ceramic fibers were developed for the protection of the space shuttle and are used as thermal insulation ceramic tiles. These materials are typically composed of 60% to 85% air and are being considered for several applications requiring thermal protection. While it is highly desirable to meaningfully characterize such materials nondestructively, until recently this act would have been considered inconceivable or impossible. It was generally assumed that higher frequencies required for NDC could not be propagated through attenuative media such as air or ultraporous materials. On the other hand, direct contact conventional wet coupling ultrasonic techniques are also incompatible with the objectives of porous media characterization, Bhardwaj (1987).[4] The only other alternative for the NDC of such materials, therefore, was to submerge them in water for ultrasound propagation. While measureable ultrasound will propagate through *water-saturaed-porous-materials,* the resultant acoustic, thus other information, would not correspond to the real stage of such a material. Obviously, what was once filled with air has been replaced by water, thus entirely altering the test material. Such methods of ultrasonic examination of porous materials cannot yield useful information relative to their characteristics.

Since the foremost requirement in NDC is the demonstration of the propagation of measurable quality ultrasound through the medium of interest, the Lockheed Corporation inquired as to the feasibility of examining *rigid porous ceramics* by Ultran's dry coupling methods. Following the initial success, several samples of such materials varying dramatically in density/porosity were submitted to our laboratory for further ultrasonic examination. The procedure used for their NDC has been described in section 1.1.

Both longitudinal and shear wave dry coupling velocity measurement techniques were applied by using 0.5MHz and 1.0MHz frequencies. By the application of *minimal* pressure on dry coupling transducers, with the test sample sandwiched in between them, it was relatively easy to propagate longitudinal waves through such materials. However, no conclusive interpretation of shear wave propagation through such materials could be established. Results of this analysis are shown in Fig. 10. Elastic moduli determined from longitudinal wave velocities were compared with those measured by conventional destructive testing, Banas (1985)[7], and are shown in Fig. 11. We conclude that not only is it possible to characterize ultraporous materials by modern ultrasound, but also that further applications of these methods on such materials will generate even more useful information relative to strength related properties.

1.5 Determination of crystal growth

A number of heat treated samples of relatively porous cristobalite polymorph of silica were investigated by dry coupling ultrasonics in order to determine the feasibility of nondestructive characterization of such materials. These samples are typically 125mm long bars and approximately 3mm thick. Velocities of longitudinal and shear waves were measured at a number of points on each sample by 6mm active area diameter and 5MHz dry coupling transducers. Results of this analysis are shown in Fig. 12. It is concluded from this data that the cristobalite content is higher at 1800^{o}F thaN at 1900^{o}F. Preliminary investigations of these materials by x-ray diffraction and scanning electron microscopy indicate that the results obtained by ultrasonic NDC are in agreement with each other.

1.6 Conclusions and Further Applications of Time Domain Ultrasonics

In this section we have demonstrated that *material-suitable acoustics (ultrasonic frequencies, pulse widths, and their bandwidths optimally applicable to a given material composition and its micro-structure)* and *material-suitable methodologies (ultrasonic methods, such as dry coupling for green stage and porous media analysis)* have been successfully developed for proper and repeatable NDC of materials. By citing several case studies, we have also demonstrated that significant ultrasonic velocities and material characteristics relationships can be established for easy and efficient NDC. Here we offer important guidelines for more practical applications of ultrasonic NDC obtained from time domain measurements.

a. When possible, for a given material to be analyzed nondestructively, first establish correlation curves analogous to Figures 5,6,7,8, and 9.

b. When it is not practical or economical to establish comprehensive and systematic relationships describing ultrasonic velocities and material parameters of interest, it is suggested that several samples of a given batch of materials be examined. For example, measure the density and velocities of ultrasound of several samples from a given batch. This exercise should generate a usable ultrasound - material parameter relationship for future use.

c. The next step should be to measure ultrasonic velocities of those materials that need to be characterized for QC/QA or for other functions. It is preferred that both longitudinal and shear wave velocities be measured. If, however, it is inconvenient to determine both velocities, then the former would suffice. Comparison of measured velocities directly to the test material parameter/s of interest should complete a given NDC objective. Once such relationships are established with respect to the reliability

and accuracy for a particular objective of characterization, then properties and/or micro-structures of test materials can be determined in a routine manner.

d. Elastic properties of materials can be easily determined once relationships in a or b have been created. Consider, for example, that by measuring the velocities of longitudinal and shear waves of an 85 % dense alumina, its density can also be obtained, Fig. 5. This information is sufficient to determine all the elastic properties of this material, as shown in Table II. This approach can be extended to any material.

e. By utilizing the sequence described here, one can characterize a material at discrete points in order to determine material homegeneity.

f. If a given material is characterized by anisotropic properties, it is desirable to measure ultrasonic parameters as functions of ultrasound propagation directions.

g. Zero degree incident beam shear wave transducers can be utilized as *acoustic polariscope,* analogous to cross polarizers in a petrographic microscope. For example, when two pure shear wave transducers are placed between an isotropic medium in such a manner that the shear wave vibration directions of the transducers are parallel to each other, then a maximum transmitted signal would be observed. If the same transducers are placed so that the shear wave vibration directions are 90^{o} apart, then a minimum or complete anulment (extinction) of the transmitted signal should be observed. On the other hand, if the test medium is anisotropic or characterized by complex arrangement of grains or fibers, such as in many modern-day composites, then the *extinction* of transmitted signal may not appear at 90^{o}. Establishment of anisotropicity vis-a-vis cross shear wave investigations can define applied or residual stresses in materials, besides reflecting upon their micro-structures. It should, however, be noted that such effects are more pronounced in visco-elastic materials and their composites, than in more elastic bodies such as ceramics. This is a subject of more inquiry, and is being investigated further, Bhardwaj (1988).[6]

2. ULTRA HIGH RESOLUTION (UHR) WITHOUT VERY HIGH FREQUENCIES (VHF)

Some of the most frequently asked questions about ultrasound for its diagnostic applications are: *How close to the test material surface can a discontinuity be resolved or how thin a material can be examined? How small a defect can be detected?* Strictly speaking, the quantitative definition of resolution and detectability must account for a given test material's chemical and physical nature with respect to applicable ultrasonic parameters. These are transducer frequency, bandwidth, pulse width, and frequency-dependence of ultrasonic attenuation. Compliance of these requirements will establish "optimum" resolution possible for a given material. Here, we briefly describe ultrasonic resolution and detectability under assumed and experimental conditions.

2.1 Ultrasonic Resolution

Resolution is the ability of a wave in distinguishing two closely lying planes or objects. In general terms, resolution can be said to increase as a function of frequency. However, resolution also directly depends upon the width of the envelope of a given wave in the time domain. In order to understand resolution from the standpoint of ultrasonic NDC, let us evaluate the possibility of highest ultrasonic resolution by considering a super-dense substrate of alumina as an example material. We assume:

Velocity of longitudinal wave: 12,000m/s
Highest applicable frequency at which there is no appreciable attenuation: 100MHz
Wavelength at 100MHz: 0.12mm
Minimum possible pulse width at 100MHz or at $\lambda/2$: 5ns
Maximum possible resolution - $\lambda/2$: 0.06mm in dense alumina at $\lambda/2$ pulse 100MHz.
If direct reflection method is used, then the time-of-flight corresponds to round-trip through the test material, thus
Maximum resolution possible is increased to 0.03mm!

These relations are defined by the well-known Bragg's Law of diffraction, i.e.,

When direct transmission method is used, $d_{min} = \lambda/2$ 5
When direct reflection method is used, $d_{min} = \lambda/4$ 6

where, d_{min} is the maximum resolution obtainable.

While we have made a case for phenomenal 30μm resolution in dense alumina, the fact is that the ultrasonic hardware to generate it at the assumed 100MHz frequency does not exist at this time. Extreme caution needs to be applied while interpreting this theoretical example. For example, while examining a material for a resolution-demanding application at a given frequency, it is very important to know the pulse width of the ultrasonic system at that frequency.

2.2 Ultrasonic Detectability

Among the users of ultrasound, it is not uncommon to find confusion while describing resolution and detectability. Often these two important terms are used interchangeably. Analogous to optical phenomenon, detectability can be defined as the ability of an ultrasonic wave to identify the smallest reflecting target or a discontinuity in an otherwise homogeneous medium through which ultrasound is propagated. Besides depending upon the wavelength, detectability is also a function of the size of an interrogating ultrasonic beam. Detectability increases as the wavelength and ultrasonic beam sizes decrease.

A general relationship describing ultrasonic detectability can be obtained from Rayleigh's diffraction-limited wave phenomenon. In an attempt to experimentally determine detectability, several tests were performed by examining artificial defects in "clean" carbon steel at 5 and 10MHz. In our estimation, the following relationship appears to yield an approximation for detectability defined as the minimum reflected area detected,

$$\Phi_{min} = K(1.22 \,.\, b.\, \lambda/64), \text{ where} \quad 7$$

K is a constant describing experimental limitations, and b is the effective dimension of the interrogating ultrasonic beam. This equation can be re-written to define detectability in terms of the diameter of the detected entity,

$$\Phi_{min} = \frac{2K(1.22 \,.\, b.\, \lambda/64)^{1/2}}{\pi}, \text{ or} \quad 8$$

$$\Phi_{min} = 0.63\, K(1.22 \,.\, b.\, \lambda/64)^{1/2} \quad 9$$

Assuming that the effective aperture of a 6mm diameter 10MHz transducer is 3.6mm (the effective aperture of a planar ultrasonic device is approximately 60% of its active area dimensions), the predicted value of detectability in carbon steel from eq. 9 is 0.13mm, not including the effects of proportionality constant K. The experimentally determined value of detectability is 0.2mm. Similarly, the predicted value of detectability by a 10MHz 12.7mm active area diameter transducer in steel is 0.18mm, while the experimentally measured value is approximately 0.4mm. Under real conditions the ideal values of detectability are reduced due to complications caused by signal-to-noise ratios, actual frequency attenuation, and other experimental conditions, denoted by constant K.

It is quite clear that the smaller the beam size, the higher the detectability. Extremely high detectability is possible through numerically controlled apertures, such as by our laboratory's Geometrical Acoustics ultrasonic devices. These are high power transducers, analogous to high power optical microscope objectives that define the beam size at the focal point as following:

$$b = \lambda/\text{n.a.}, \text{ where} \qquad 10$$

$$\text{n.a. (numerical aperture)} = 2 \sin \alpha \text{ , when} \qquad 11$$

$$\alpha \text{ (angular aperture)} = \sin^{-} d/f, \text{ where} \qquad 12$$

d is the diameter of active transducer, and f is its focal length in a given medium of ultrasound transmission. By substituting b from eq. 10 into eq. 9, we can describe an ideal definition for detectability in terms of the diameter of the detected entity,

$$\Phi = 0.63\, K\, (1.22\, \lambda^2/64\, .\, \text{n.a.})^{1/2} \qquad 13$$

Again, for the sake of argument, let us assume that an ultrasonic device of 100MHz is characterized by maximum numerical aperture of 2. This will yield the maximum detectability of internal reflectors (grain or pore size, grain boundaries, etc.) in dense alumina corresponding to 7μm from eq. 13! We must state that these are ideal numbers under ideal conditions that do not prevail in the real world. However, one comment about detectability is in order, i.e., it is not dependent upon the pulse width of interrogating ultrasound as is the resolution.

Here, we have only described spatial or bulk detectability of an interrogating ultrasonic beam. This should not be confused with surfacial detectability. For example, if surface detectability needs to be established, such as by immersing a test sample in water, then the corresponding wavelength in water should be used. In dense alumina the maximum surface detectability by a 100MHz transducer of numerical aperture 2 is 0.9μm!

The relationships describing detectability here are approximations and to a degree experimentally investigated at relatively lower frequencies on the smallest size artificial defects easily producible. However, these relationships should be evaluated further in order to establish their validity for practical NDC.

2.3 Practical UHR Without VHF

Due to misleading and confusing information proliferated by NonDestructive Testing (NDT) users and manufacturers, it is commonly believed that by *increasing the frequency of ultrasound, higher resolution is achieved.* This statement by defintion correct.

However, indiscriminate increment of frequency cannot universally improve resolution requirements. There are several factors that complicate this issue. Very High Frequency (VHF) ultrasonics - generally beyond 50MHz - is far from being perfect from the standpoint of VHF ultrasonic excitation and amplification electronics, and VHF ultrasound does not automatically mean *short pulse widths,* a pre-requisite for high resolution observed in section 2.1. Furthermore, while considering the extreme resolution of defects or of thickness of a given material one must understand two limiting factors: frequency dependence of ultrasound attenuation/absorption, and material dependence of ultrasound attenuation/absorption. The former describes scatter or absorption-limited behavior of a test medium as a function of varying frequencies, Bhardwaj (1987)[4]. The latter determines frequency-limited behavior of a given ultrasound frequency as a function of varying test materials, Bhardwaj (1988)[8]. In order to present a complete picture of ultrasonic NDC for diverse and complex modern materials - from highly dense to highly porous, and from homogeneous to heterogeneous - these factors must be clearly understood.

In some VHF applications of ultrasound, such as in *high resolution acoustic microscopes,* Ultra High Resolution (UHR) describing sub-surfacial images in micron regions are claimed. It should, however, be noted that not only are such mechanisms limited to the depths to which materials can be examined, but also that the pulse widths of interrogating frequencies (into 100s of megaherts) are typically several wavelengths. Importance of pulse width in NDC has been covered substantially by Ultran (1987)[9] and Bhardwaj (1987)[4]. Here we briefly describe the relationship of the pulse width with resolution and offer several examples of UHR without VHF.

Pulse width of an ultrasonic transducer is described by the amount of time its pulse occupies in a time domain trace. For example, at a given frequency the pulse width will increase as the oscillations or the number of wavelengths of the vibrating transducer increase. Imagine the ringing of a bell or that of a musician's cymbal! Excessive ringing causes loss of time or distance resolution, and it must be curbed for high resolution ultrasonic measurements. The limit to which the pulse width of a transducer can be decreased is half the wavelength at a given transducer frequency. In an attempt to achieve this requirement, several years ago our laboratory developed λ-series transducers characterized by pulse widths within 0.5λ to 1.0λ. Fig. 13 shows the pulse response from 10MHz and 5MHz λ-series transducers. The theoretical minimum pulse of a 10MHz is 50ns, while for a 5MHz it is 100ns. From the observations in Fig. 13, we obtain practically achievable pulse widths of 50ns and 120ns for 10MHz and 5MHz λ-series transducers, respectively. In the following sections we show the applications of such devices for extreme resolution and defect detectability.

2.4 Measurement of Thin Materials and Coatings

In order to demonstrate the applicability of extraordinary resolving capabilities of λ-series ultrasonics, a delayed 10MHz and 6mm active area transducer was used. The physical arrangement of the transducer with test material is shown in Fig. 14. Since only dense and impervious materials were examined here, a thin layer of glycerine was used as couplant between the transducer delay and test materials interface. We would, however, like to point out that by using dry coupling designs of λ-series transducers, the same results are obtained with a slightly reduced resolution.

Fig. 15 is an rf A-scan obtained from 1.0mm thick BeO substrate by direct reflection method with a delayed 10MHz, 6mm active area diameter λ-series transducer. Observe 100% resolution of the top and bottom surfaces of this material. In Fig. 15, the left hand cursor is

placed at the delay-BeO interface, and the right hand cursor is at BeO - ambient interface. The measured round trip time-of-flight is 176.5ns, yielding longitudinal wave velocity of 11,330m/s. Since the pulse width of the transducer used is short enough, even thinner samples of BeO or like materials can be reliably examined by using this method. Considering the fact that dense oxides, carbides, nitrides, and borides are typically long wavelength materials (BeO at 10MHz being 1.13mm), it is particularly encouraging to note that the relatively low 10MHz frequency, but of very short pulse width, enables extraordinary high resolution without the applications of VHF.

In order to characterize a thin coating of a drilling diamond tool - deposited on a WC substrate - an arrangement similar to the one shown in Fig. 14 was used. Ultrasound from a delayed 10MHz and 6mm active area diameter λ-series transducer was propagated from the WC side, as shown in Fig. 16. The resulting ultrasonic signal is shown in Fig. 17. Here, the left cursor is at WC - diamond interface and the right one is at diamond - ambient interface. The round trip time-of-flight through 0.86mm thick diamond is 140ns, yielding 12,285m/s velocity of longitudinal waves. As a reference the velocity of WC measured from this specimen is 6,840m/s.

Fig. 18 is a multi-trace rf A-scan from bonded (top) and partially bonded conditions of barium titanate with glass in a multi-layer ferrite composite obtained by the λ-series transducers used previously. Note that when the ceramic is bonded - top trace - the interface between glass and ceramic (left indication) is clearly defined from glass and ambient interface (right indication). When there is a partial or complete disbond at the glass - ceramic interface, most of the ultrasonic energy is reflected directly from this interface, thus minimizing the reflection from glass - ambient interface, Fig. 18, bottom trace.

2.5 Measurement and Detection of Shallow Sub-surface Defects

In order to demonstrate simultaneous resolution and detectability of very shallow sub-surface defects, an artificial defect, 1.0mm diameter, located at 0.4mm in an aircraft quality aluminum was characterized. This was accomplished by water delay or immersion method, utilizing a λ-series transducer of 10MHz frequency, 6.0mm active area diameter and 19mm point focus in water. The top trace in Fig. 19 corresponds to the defect-free region in the test sample, thus only showing water - aluminum interface. The bottom trace clearly shows the appearance of the shallow sub-surface defect along with several multiples.

2.6 Conclusions and Further Applications of λ-Series Ultrasonics

λ-series transducers were developed for two major reasons: to reduce the transducer impulse response in such a manner that the resultant pulse width would correspond to the *utmost minimum*, and to enhance high resolution ultrasonics without the cumbersome and limited applications of Very High Frequencies (VHF, generally beyond 50MHz). We have demonstrated the practical applications of this development in thickness/thinness and defect characterization. One well-versed in ultrasonic NDC would appreciate that the examples shown here could not be easily obtained by other high resolution methods utilizing relatively high frequencies. Besides the cited applications of λ-series ultrasonics, there are several other important features and applications of this dramatic development in NDC. These are listed along with our recommendations.

a. Highly controlled pulse widths, corresponding to λ/2.

b. Ultrasound beam collimation.

c. Virtual elimination of side-lobing phenomenon.

d. Near absence of the deleterious effects of near field.

e. Highly symmetrical and uniform field of ultrasound.

f. White frequency spectra for Wideband Ultrasonic Spectroscopy (WUS).

For further details on λ-series transducers and their applications, please refer to Ultran (1982).[10]

3. QUANTITATIVE ULTRASONIC IMAGING

By measuring the strengths of reflected or transmitted ultrasonic signals from a test material as a function of transducer location, it is possible to generate planar image corresponding to the internal characteristics of the material. Such images are commonly generated by immersion scanning methods and are popularly known as C-scans. The pictorial quality of such scans is directly dependent upon the accuracy and precision of mechanical system driving the transducer, homogeneity and frequency absorption of the immersion medium, the acoustic and field characteristics of the interrogating transducer, the capability of ultrasonic electronic system in driving the transducer, and in the detection and amplification of signals being monitored for C-scanning. Ultrasonic C-scanning has been known for more than two decades in the metals and aircraft industries. Necessitated by the utgency for NDC, the conventional C-scanning has undergone substantial advancements during the recent years. Coupled with advanced transducers, broad bandwidth ultrasonic amplifiers, and precision mechanical systems, C-scanning methods have been revolutionized with the advent of extraordinary applications of computer technology. In this section we describe the progress made in our laboratory in the area of ultrasonic imaging and show several examples of this technique for advanced materials characterization applications.

3.1 Experimental techniques

In order to conduct comprehensive ultrasonic imaging of materials, Ultran's NDC 7000 system was used. This system is the combination of a variety of analog and digital ultrasonic and computer hardware and software, including an immersion raster scanning mechanical system. A schematic layout of NDC 7000 is shown in Fig. 20. This system is fully compatible with an IBM PC (AT) or similar systems controller. The examples of imagery that follows, utilized high resolution ultrasonic transducers described in section 2. Brief description and functions of various important elements of this system are as following:

a. SFT 4001: This is a programmable ultrasonic PCB, including a software PULSET which is used for control and operation of ultrasonic parameters.

b. SFT 4000: It is an analog-to-digital converter PCB, including software SOFRASCOPE, which transforms the computer screen into a virtual oscilloscope. SFT 4001 and SFT 4000 can be used up to 10MHz ultrasonic frequencies by utilizing SOFRASCOPE. With an external oscilloscope, these PCBs can be used to 20MHz frequencies.

c. SFT 3000 & 3001: These are 3-axes indexer PCBs for the motorized controls of an immersion scanner and include software TRANSCAN. This software is used for acquiring a standard C-scan data.

d. HF 400: It is an analog high frequency transducer excitation and amplification system which can be utilized with SFT 4000 when ultrasonic frequencies up to 35MHz are used. When this system is used, the functions of SFT 4001 are by-passed.

e. TEKTRONIX 2432 Oscilloscope: This is a multi-functional 300MHz digital storage oscilloscope used for signal monitoring, and time and frequency domain analysis.

f. TEKTRONIX PEP 301 Systems Controller: It is a 16MHz Intel 80386 system with 80387 coprocessor. This system drives, operates, and analyzes all ultrasonic, mechanical, and other parameters.

g. ULTIMAGE: It is a powerful and extremely fast software for digital and spectroscopic analysis of C-scan data acquired by TRANSCAN. ULTIMAGE facilitates filtering of acquired data for image refinement and for quantitative digital analysis of images.

3.2 Imaging for Minute Pores in a Homogeneous Medium:

An artificially created 75μm diameter defect located at 0.25mm in a 0.5mm thick specimen of carbon steel (made by the Timken Company's R & D Center) was analyzed as per the procedures described in section 3.1. Fig. 21 is the representation of a C-scan from this sample which does not reveal the tiny defect. If data was interpreted from this analysis, the sample studied would be classified as a homogeneous material. However, an ULTIMAGE refined of this image, Fig. 22, clearly shows the appearance of a 75μm defect at the upper left hand corner. The transducer used is a λ-series with 6mm active area diameter, 10MHz frequency, and 19mm point focus in water. According to eq. 13, the detectability in steel by this device is 60μm, and experimentally detected value here is 75μm, a reasonably good comparison. The specimen of steel analyzed here also contained two more artificial defects, measuring 50μm and 25μm diameters. Under the experimental conditions and the 10MHz transducer used in this analysis, these defects could not be identified. On the other hand, with a 30MHz transducer of a numerical aperture 1, 25μm and 50μm defects in steel could be detected.

3.3 Imaging of Micro-structure in Ceramics:

Figures 23 and 24 are respectively planar and 3-D images of a crystalline glass, pictorially exhibiting micro-structure of the sample. Digital cross-sectional profiles can be used to quantify variations caused by chemical composition and/or micro-structure in the acoustic levels of the signals.

Fig. 25 is an ultrasonic image of a commercial sample of Lead Zirconate-Lead Titanate, showing material heterogeneity, presumably due to partial chemical reactions. This is also indicated by cross-sectional profiles of digital acoustic pressure (top and right hand curves of Fig. 25).

Fig. 26 is another example of heterogeneity in a ceramic, in this case a 92.3% sintered alumina dtermined by ultrasonic imaging. Observe subtle density variations - enhanced by colored rings. If the density of yellow bands is 92.3%, then the digitally determined value of the lesser dense green region is approximately 83%. Similar investigations on ceramics

have been reported by Generazio, Roth, and Baaklini (1988)[11] by utilizing very high ultrasonic frequencies.

Fig. 27 and 28 are, respectively, an ordinary C-scan and an ULTIMAGE refined ultrasonic image of a lithia-alumina-silica composite. It is quite evident that the C-scan alone is unable to describe the fine details of micro-structure, while digital signal processing can, Fig. 28. For further details, see the captions of these figures.

3.4 Imaging of Fiber-Reinforced Plastics:

Fig. 29 is an enhanced ultrasonic image of a 1.4mm graphite fiber reinforced plastic composite that is artificially damaged by impact. This analysis was performed by monitoring the reflection of ultrasound from the far side of the test sample. Observe clean demarcation of the geometry of impacted region, along with the appearance of fiber orientation. Fig. 30 shows the results of the same specimen, however, in this case the internal scatter from the sample was monitored while acquiring the data. The geometry of impact damage in this case corresponds to the inner region of the composite. Fig. 30 further reveals fiber damage and delaminations in the inner region of this sample.

Fig. 31 is another example of a composite, composed of glass fiber-reinforced plastic. It is a 6mm thick sample that has been catastrophically damaged by a 76mm target. Observe the effects of this impact upon the damage in the central region, while the outer four triangles represent relatively lesser, or undamaged regions.

4. CONCLUSIONS

In this paper we have described significant developments in ultrasonic NDC science and technology for material property determination and for practical imaging or microscopy for texture and other parameters evaluation. We have also outlined important ultrasonic considerations, such as the relationships of transducer characteristics with respect to specific test materials characterization objectives. A number of examples and concepts have been provided in order to demonstrate the applicability of ultrasound as a viable and reliable tool for nondestructive characterization of materials. We have also shown that the modern advancements of technology can be gainfully applied at various stages of materials processing, such as during their development and manufacture, and under *in situ* conditions. The subject covered in this paper is the direct result of the combined ambition of our laboratory, i.e., to develop and to present ultrasonic NDC analogous to any other currently accepted characterization tool in the industry and research laboratories. We conclude that this development is by-and-large complete and comprehensive. The scope of our presentation will be undoubtedly enhanced by its applications at QC/QA functions, as well as by further refinement and correlations of modern ultrasonic observations by the advanced users and developers of NDC techniques.

ACKNOWLEDGEMENTS

Partial support for the work reported in this paper was received from a Pennsylvania Ben Franklin Partnership Grant #11a. The author is indebted for valuable contributions to Charles J. Valenza, Director Transducer Technology, Arun Madhav, R & D Scientist, and Anant S. Trivedi, Instruments Consultant, all of Ultran Laboratories. We also recognize Pierre Potet, CEDIP, Paris, France, for the spectacular development of the ULTIMAGE software, and Bernard Audenard, SOFRATEST, Ecquevilly, France, for the advances in digital ultrasonics. Professors Amar S. Bhalla and David J. Green of Penn State University have frequently

assisted us in special sample requirements as well as for data interpretation. Mini S. Bhardwaj has tirelessly critiqued the author's work in order to keep the high standards of our laboratory.

REFERENCES

1. Bhardwaj, M.C., "Principles and Methods of Ultrasonic Characterization of Materials," Adv. Cer. Mat., vol. 1, #4 (1986).

2. Vary, A., (Editor), "Materials Analysis by Ultrasonics," Proceedings of conference of the same title, Noyes Data Corporation, Ridge Park, NJ (1987).

3. Thompson, D.O. and Chimenti, D.E., (Editors), "Review of Progress in Quantitative Nondestructive Evaluation," in the proceedings of annual symposia of the same title, Vols. 1 to 7, Plenum Press, New York (1982-88).

4. Bhardwaj, M.C., "Fundamental Developments in Ultrasonics for Advanced NDC," Proceedings of a conference on Nondestructive testing of High Performance Ceramics, Boston, Mass., Am. Cer. Soc. (1987).

5. Vary, A., "Ultrasonic Measurements of Materials Properties," in Research Techniques in Nondestructive Testing, vol. IV, Academic Press, New York, (1980).

6. Bhardwaj, M.C., "Mechanism of Shear Wave Propagation: an Experimental Investigation," in process (1988).

7. Banas, R.P., Creedon, J.F., and Cunnington, G.R., "Thermophysical and Mechanical Properties of the HTP Family of Rigid Ceramic Insulation Materials," AIAA 20th Thermophysics Conference, Williamsburg, VA June 1985.

8. Bhardwaj, M.C., Modern Ultrasonic NDC: Its Importance, Progress, and Practice in the World of Materials," submitted to Adv. Mat. Proc. (1988).

9. Ultran Laboratories, Inc., "Ultrasonic Nondestructive Characterization: Prospects for Materials and Processes," an Ultran Laboratories Publication #EPN 107 (1987).

10. Ultran Laboratories, Inc., "Lambda Transducers: Their Features and Applications in Nondestructive Characterization of Materials," an Ultran Laboratories, Inc. Publication #EPN 104 (1982).

11. Generazio, E.R., Roth, D.J., and Baaklini, G.Y., "Acoustic Imaging of Subtle Porosity Variations in Ceramics," Mat. Eval., vol. 46, #10 (1988).

END TECHNICAL TEXT

MCB:cbm October 1988

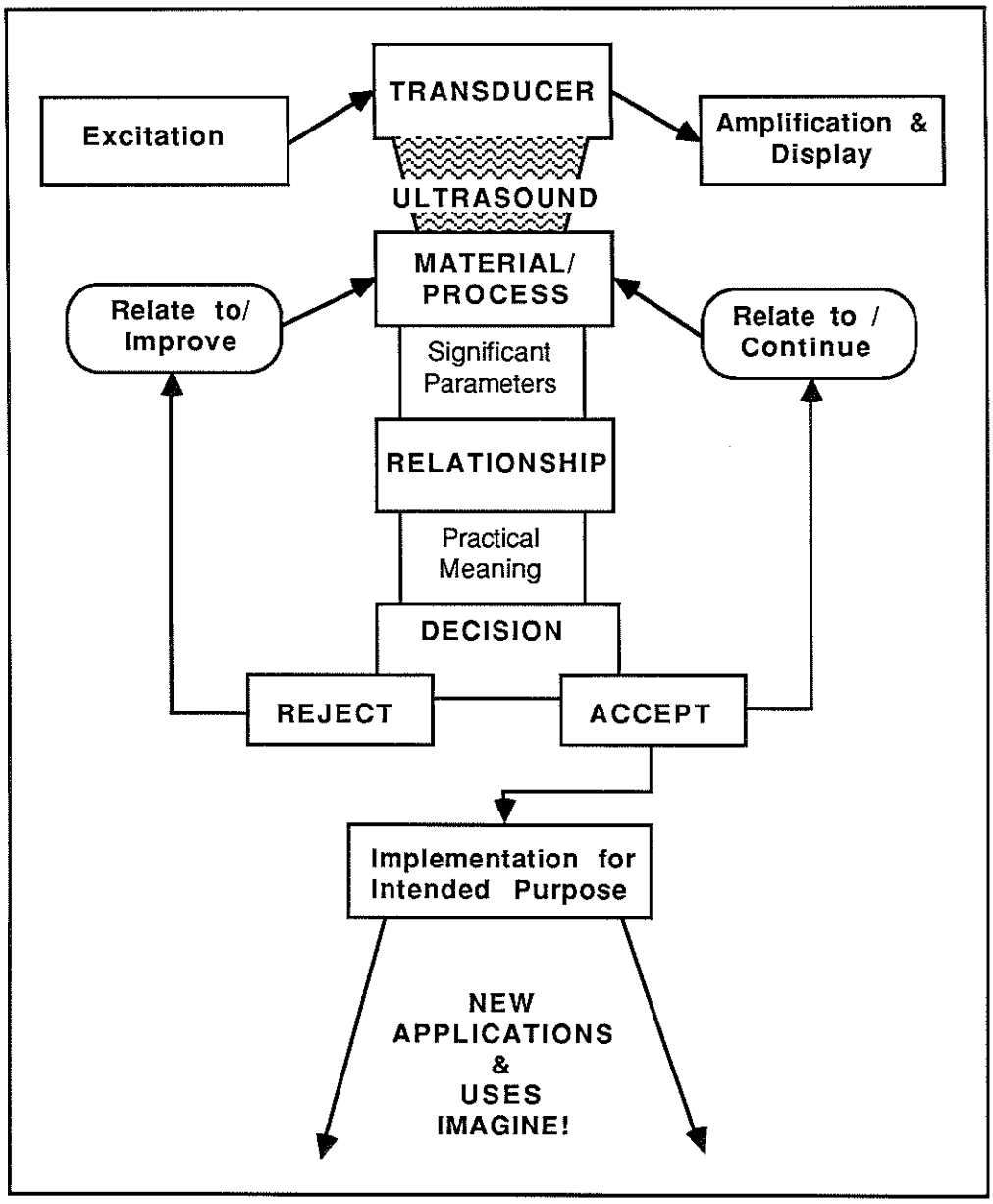

Fig. 1. A perspective on Ultrasonic Characterization of Materials showing the Significance of Ultrasonic NDC for Materials Manufacturing Process.

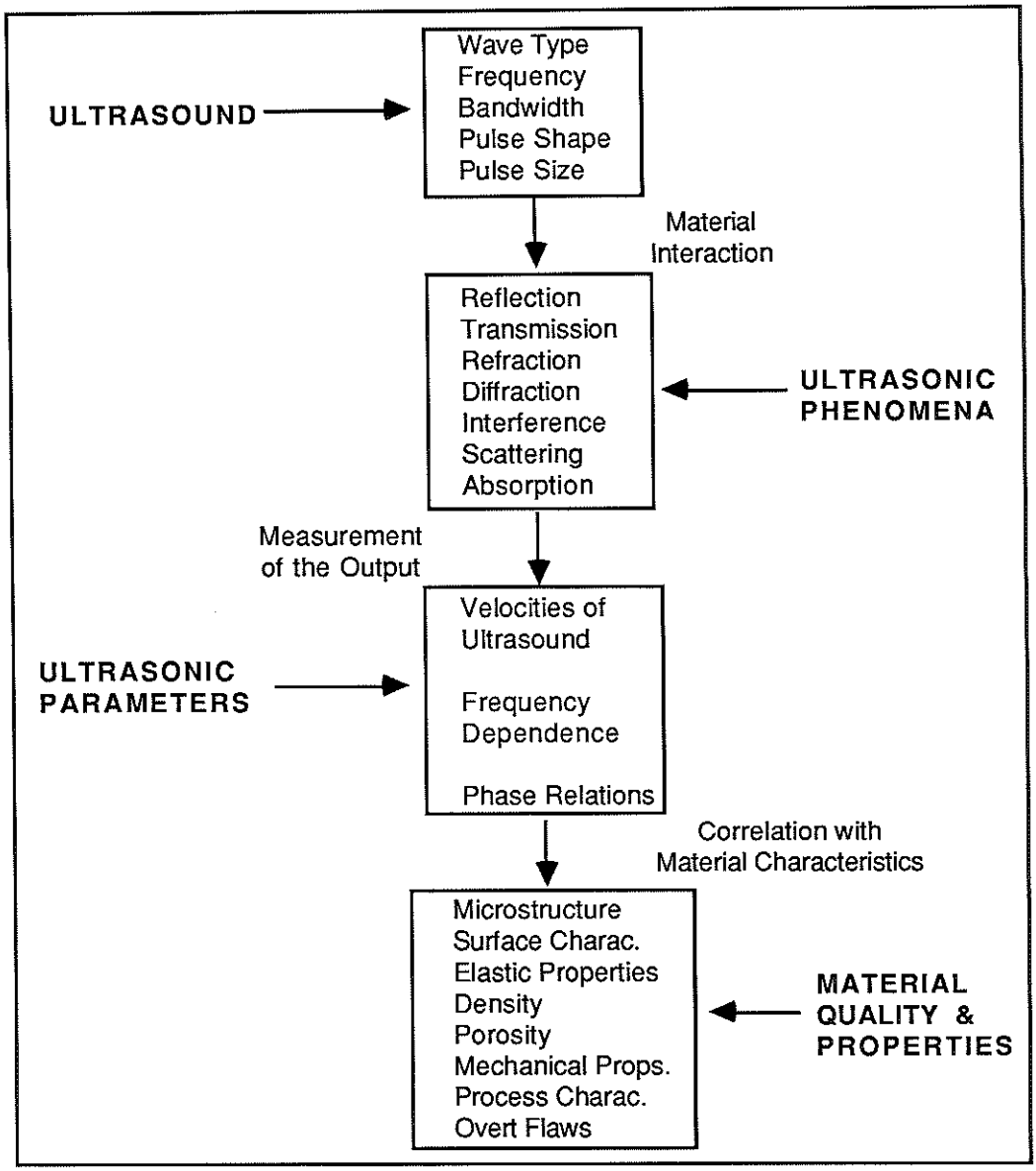

Fig. 2. Principles of Ultrasonic Nondestructive Characterization showing the relationships between the characteristics of ultrasound and its measured parameters with test material quality and properties.

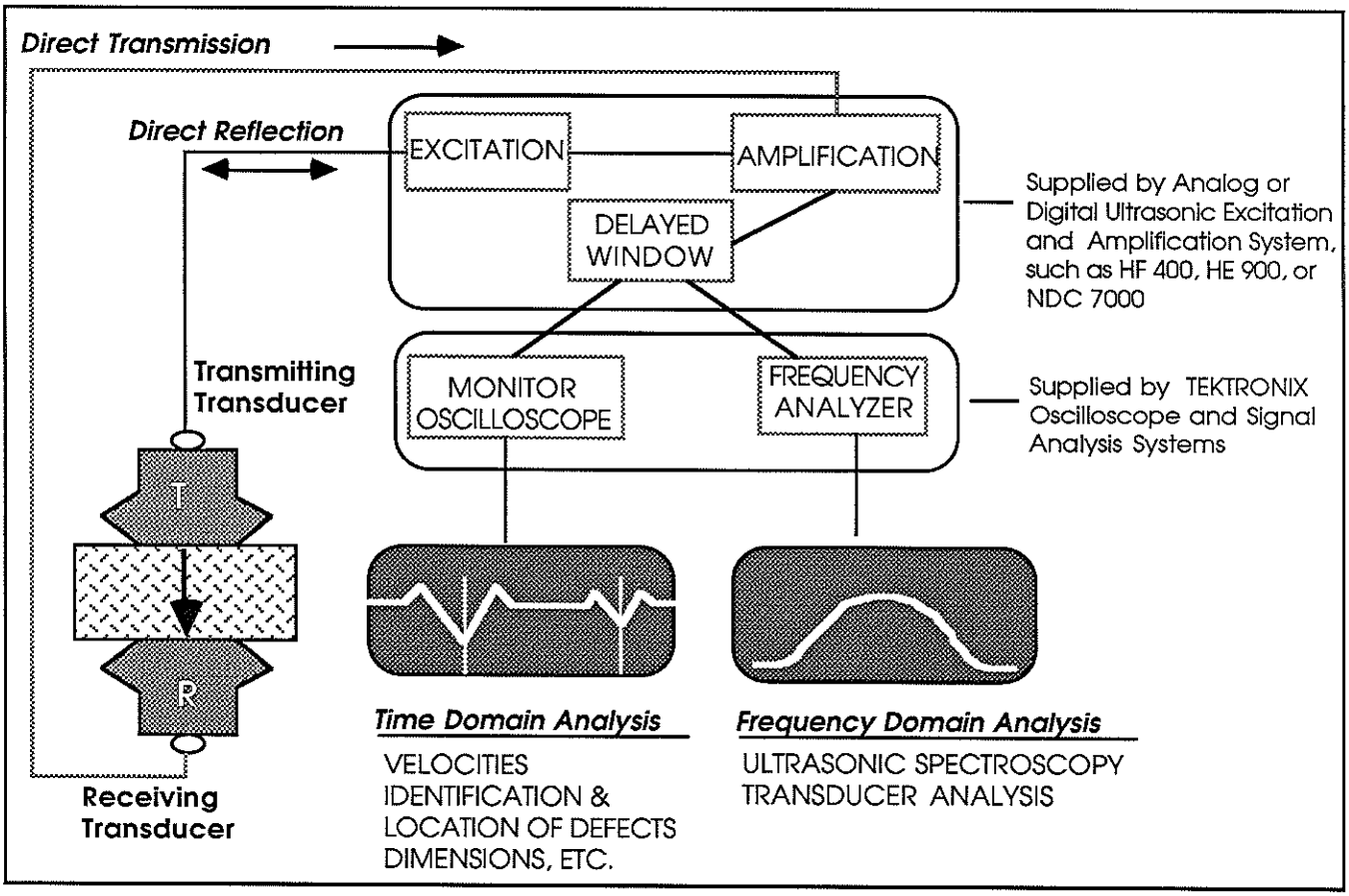

Fig. 3. A schematic layout showing pulsed ultrasonic set up for time and frequency domain ultrasonic characterization of materials.

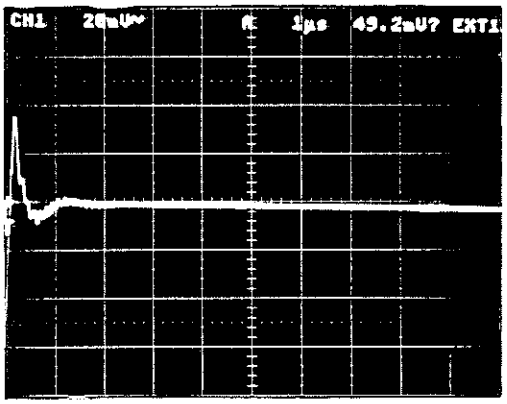

Fig. 4a.
Triggered Oscilloscope Trace, without Transducers.

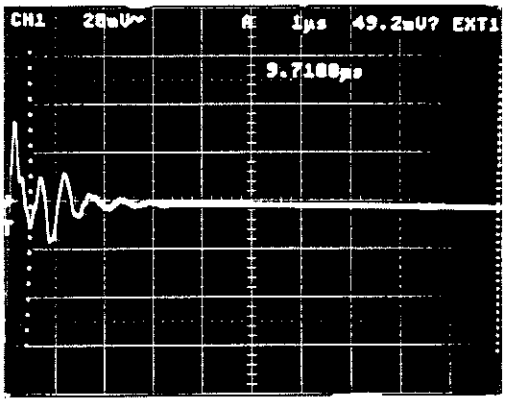

Fig. 4b.
Oscilloscope Trace with two Transducers coupled together.

Note the location of left hand cursor, adjusted at the transmitted signal from transducers matching layers. This cursor establishes a reference or "0" point from where time-of-flight measurements are to be made.

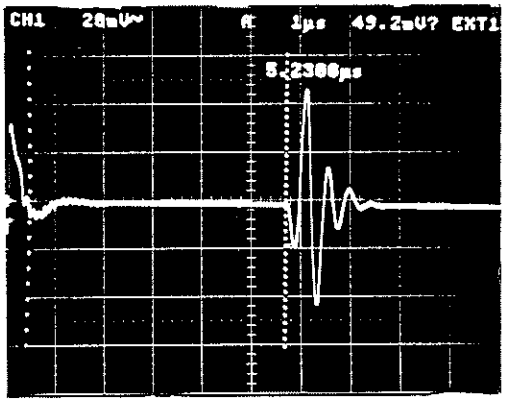

fig. 4c.
Oscilloscope Trace with test material sandwiched between the two transducers.

The position of left hand cursor is unchanged. The right hand cursor is adjusted at the trailing edge of the transmitted signal from the test material.

The actual time-of-flight is automatically measured between the two cursors and displayed on the oscilloscope screen - in the present case it is 5.23 µs.

Fig. 4. Systematic sequence for accurate velocity measurement by direct transmission method.

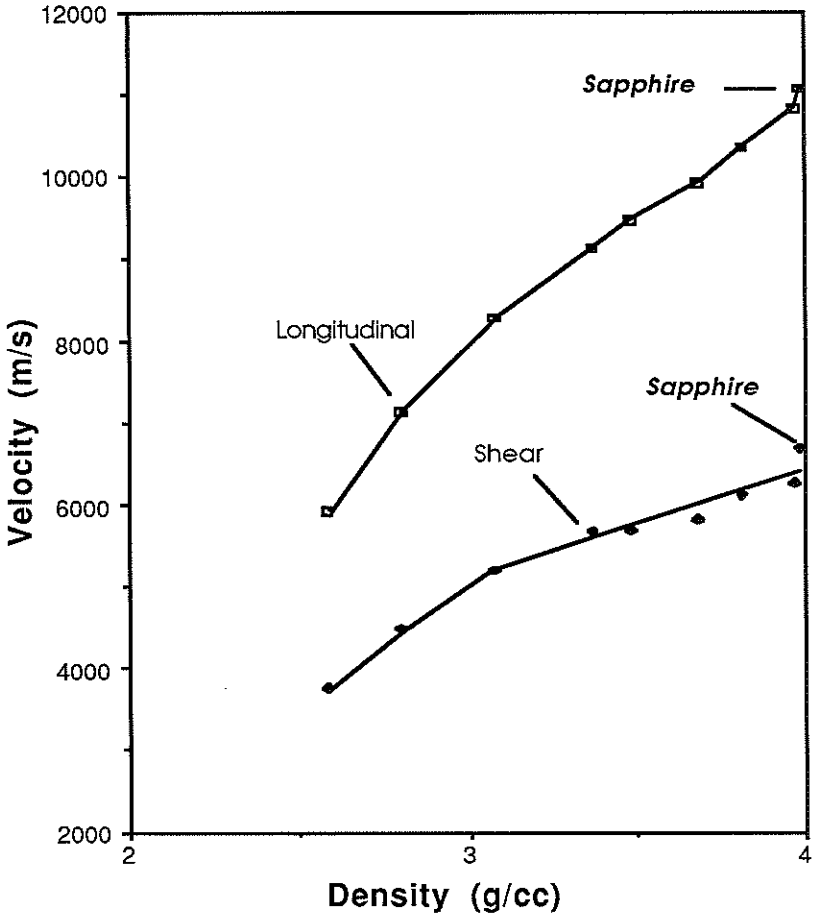

Fig. 5. Relationship between the density of sintered alumina with velocities of longitudinal and shear waves determined by Dry Coupling Direct Transmission method.

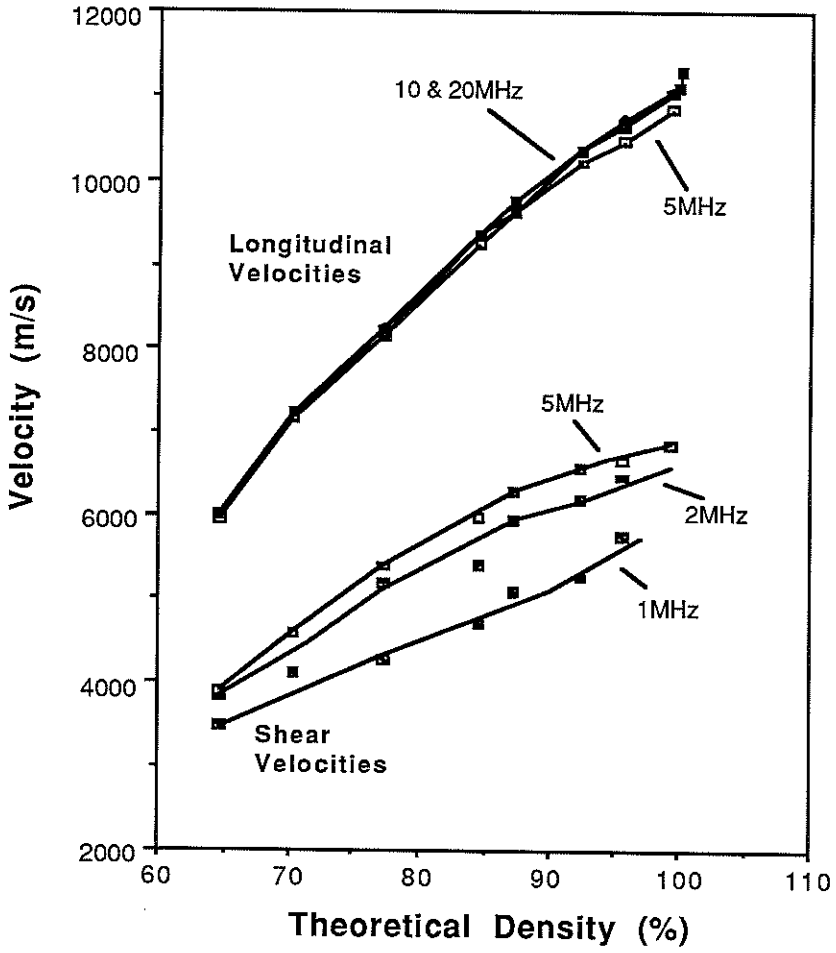

Fig. 6. Longitudinal and shear velocities of sintered alumina as functions of varying frequencies. All measurements were carried out by Dry Coupling Direct Transmission method.

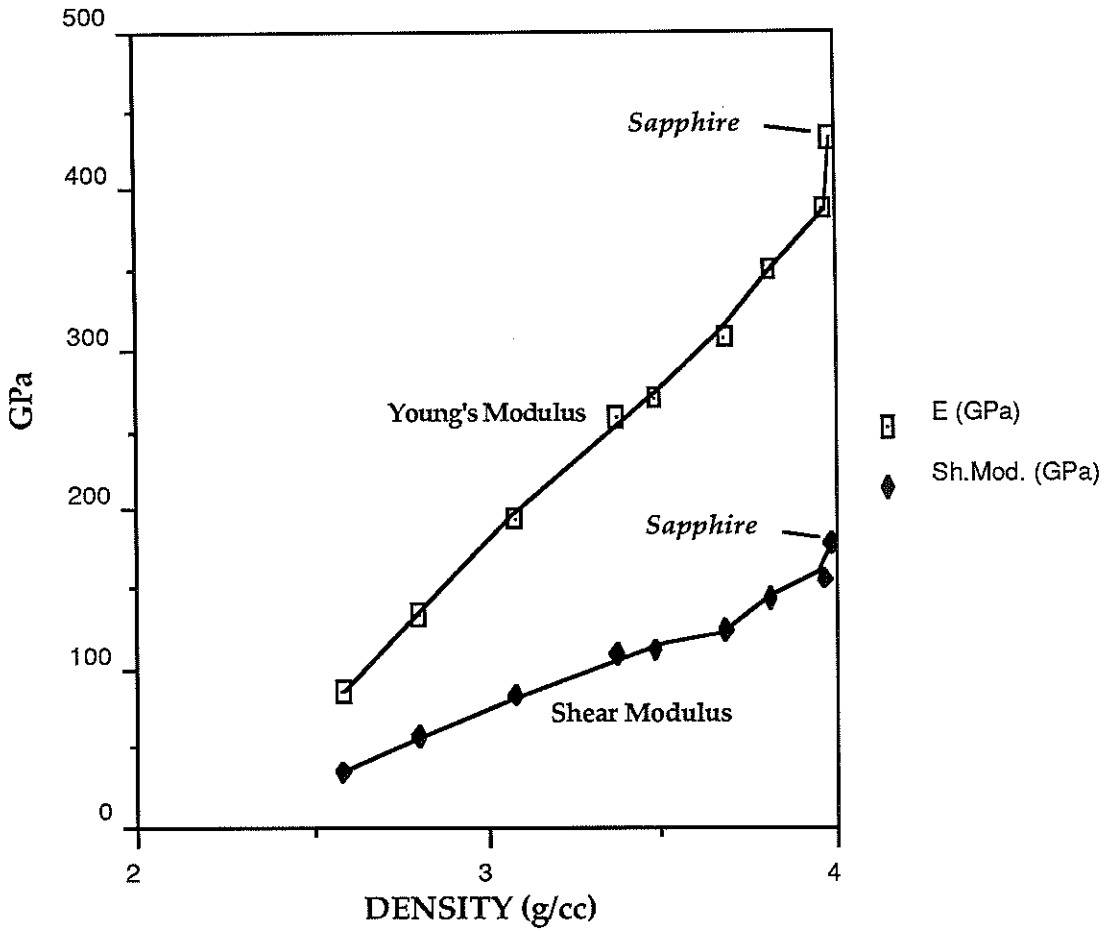

Fig. 7. Elastic and Shear Moduli of sintered alumina determined from the data in Fig. 5.

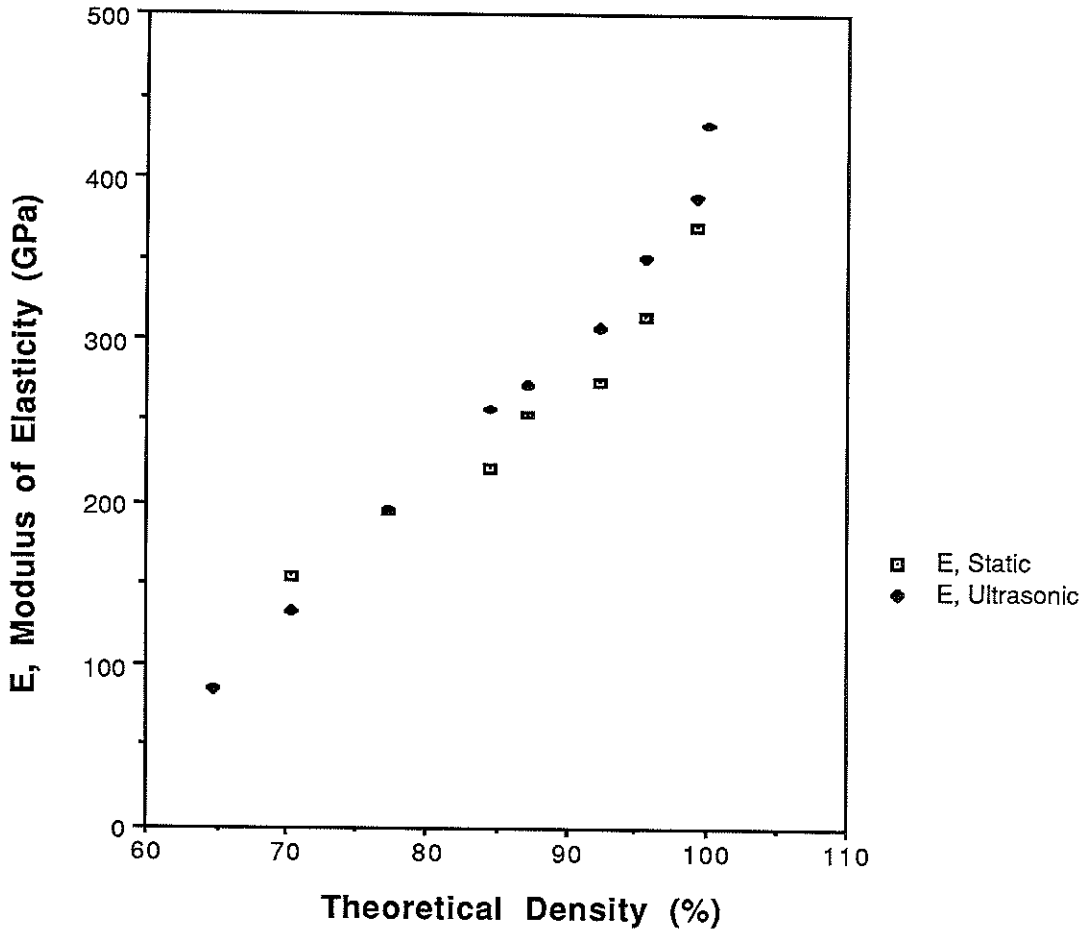

Fig. 8. Comparison of destructively (4-point bending method) and nondestructively (ultrasonic dry coupling direct transmission method) determined modulus of elasticity as a function of density of sintered alumina.

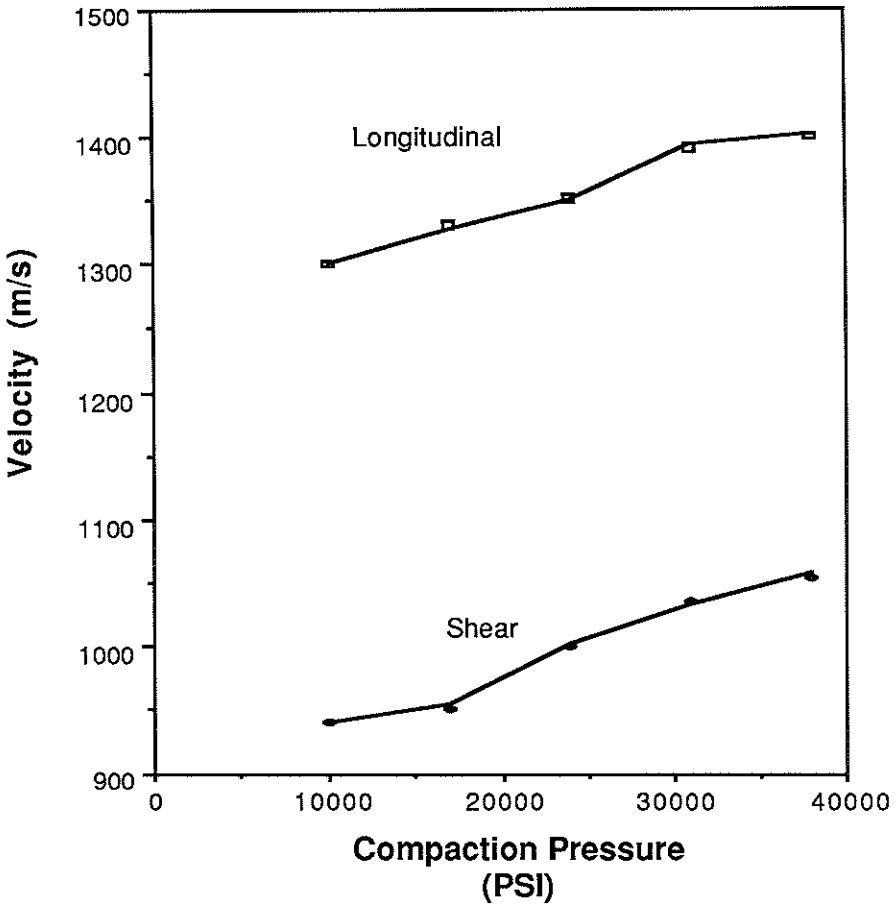

Fig. 9. Ultrasonic characterization of green stage ceramics. Relationship between compaction pressure of a green state alumina - comprising of alumina powder and organic binder - with the velocities of longitudinal and shear waves. All measurements were made by Dry Coupling Direct Transmission method.

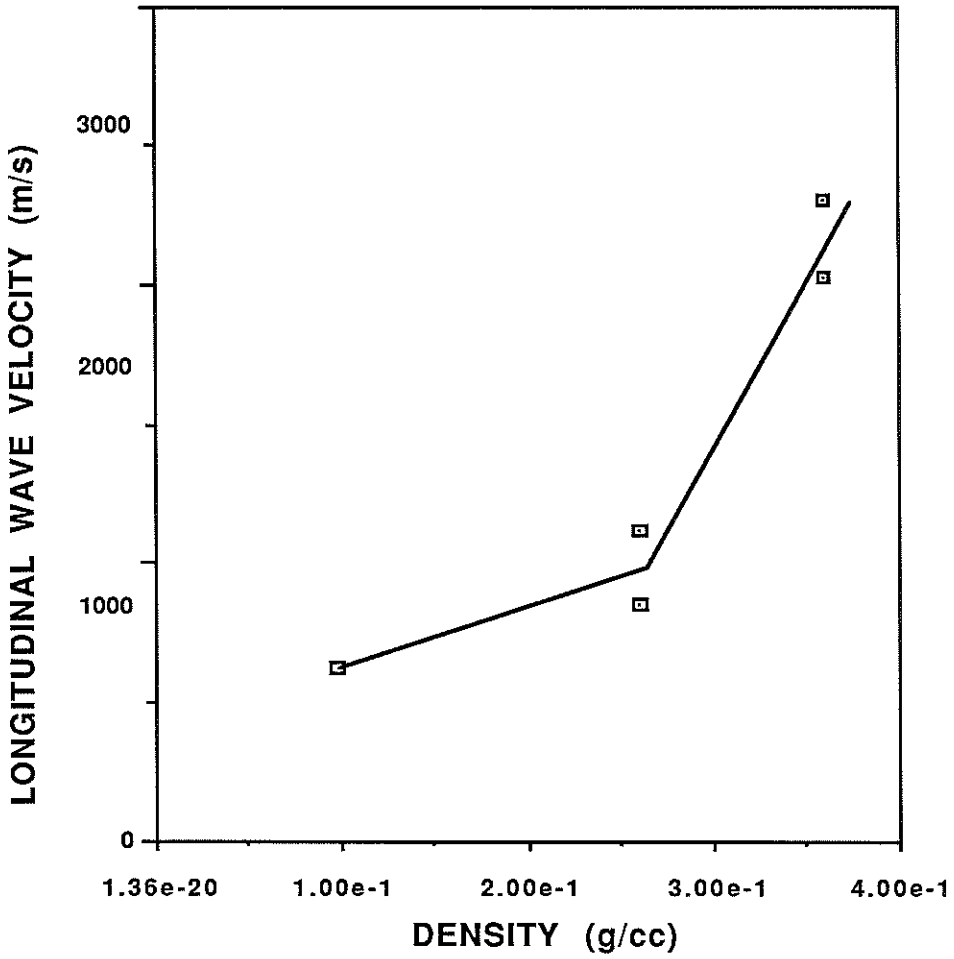

FIG. 10. Characterization of Ultra Porous Ceramics.

Relationship between longitudinal wave velocity and density of "ultra" porous (60 to 85% porosity) rigid ceramics determined by Dry Coupling ultrasonic methods.

Source of samples: Lockheed Corporation.

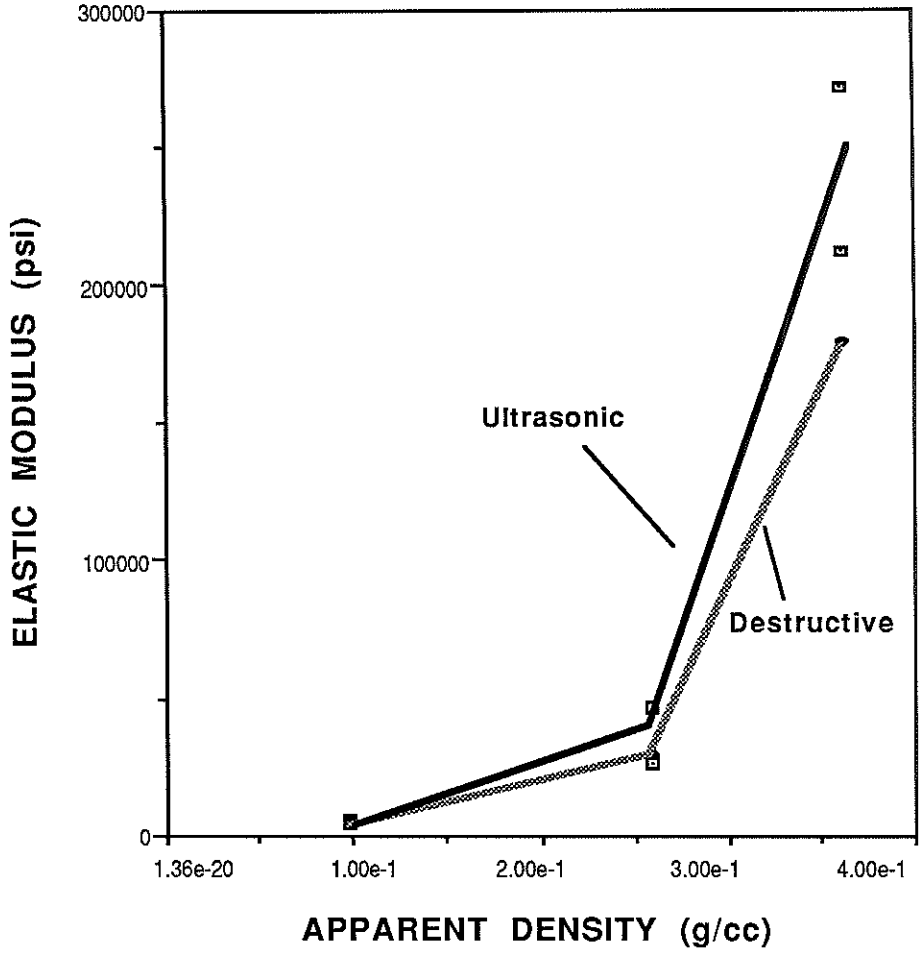

Fig. 11. Comparison of destructively and ultrasonically determined elastic moduli of "ultra" porous rigid ceramic fibers in thickness direction as functions of density.

Source of samples: Lockheed Corporation.

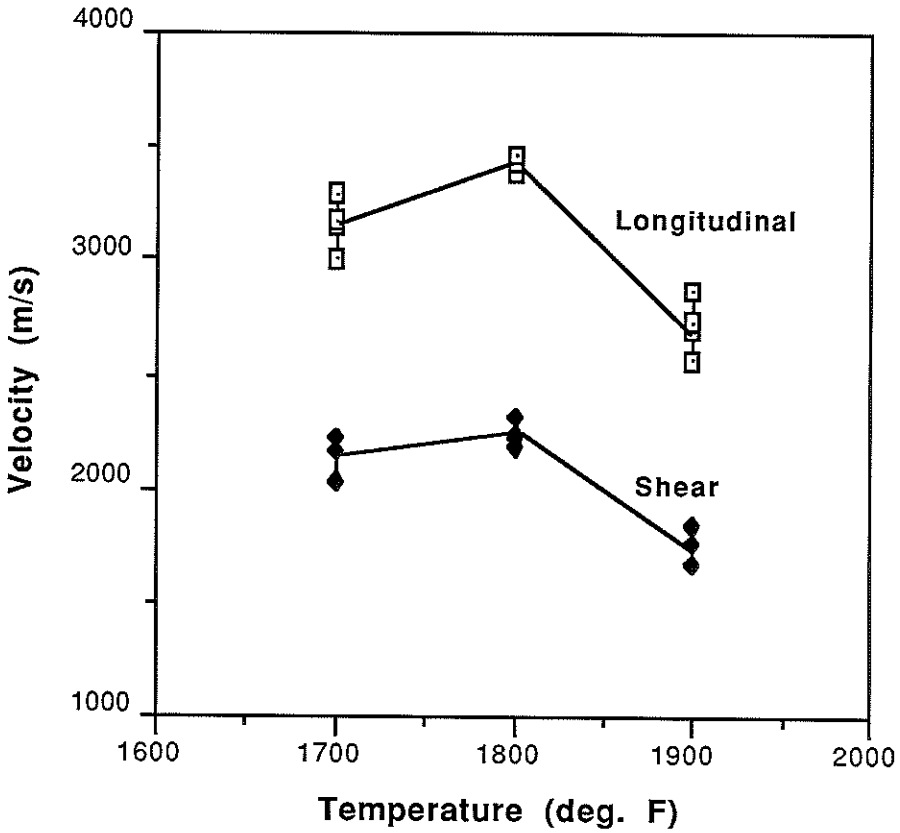

Fig. 12. Determination of cristobalite content as a function of temperature by the measurement of longitudinal and shear wave velocities. All measurements were carried out by Dry Coupling Direct Transmission method.

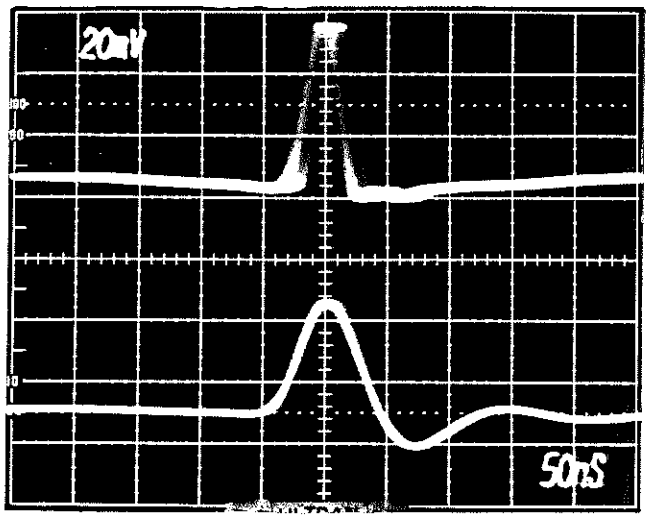

Fig. 13. Typical impulse response of λ- series transducers, exhibiting "shortest" possible pulse widths.

Top Trace: Pulse width and shape of a 10MHzλ - series transducer.
Measured value: approximately 50ns.
Theoretical$\lambda/2$ pulse width: 50ns.

Bottom Trace: Pulse width and shape of a 5MHz λ- series transducer.
Measured value: approximately 120ns.
Theoretical $\lambda/2$ pulse width: 100ns.

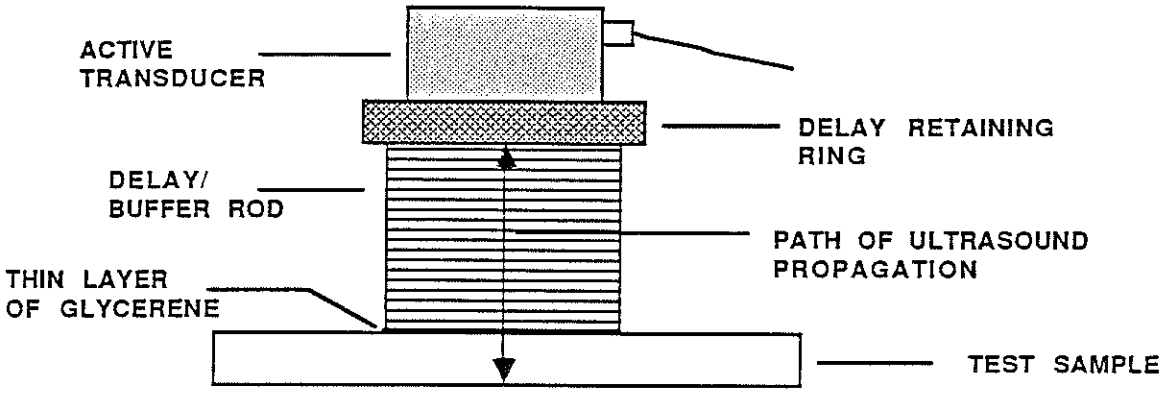

FIG. 14. Coupling of a delay line λ- series transducer to the test material surface used to demonstrate Ultra High Resolution (UHR) without Very High Frequencies (VHF).

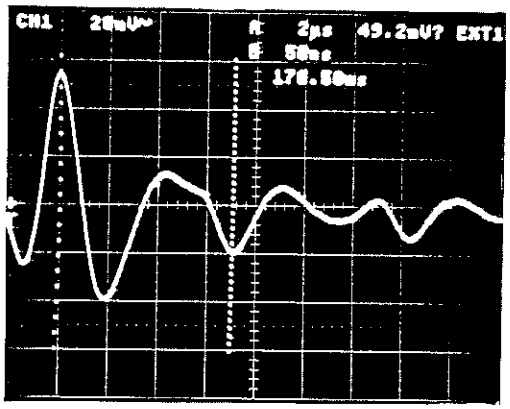

Fig. 15. 100% resolution of top and bottom surfaces of a 1.0mm dense BeO substrate obtained by a delayed contact λ - series transducer, nominally 10MHz and 6mm active area diameter. The left hand cursor is at the delay - BeO interface, and the right hand cursor is at BeO - ambient interface. Measured round trip time-of-flight: 176.5ns.
Measured velocity of ultrasound: 11,330m/s.

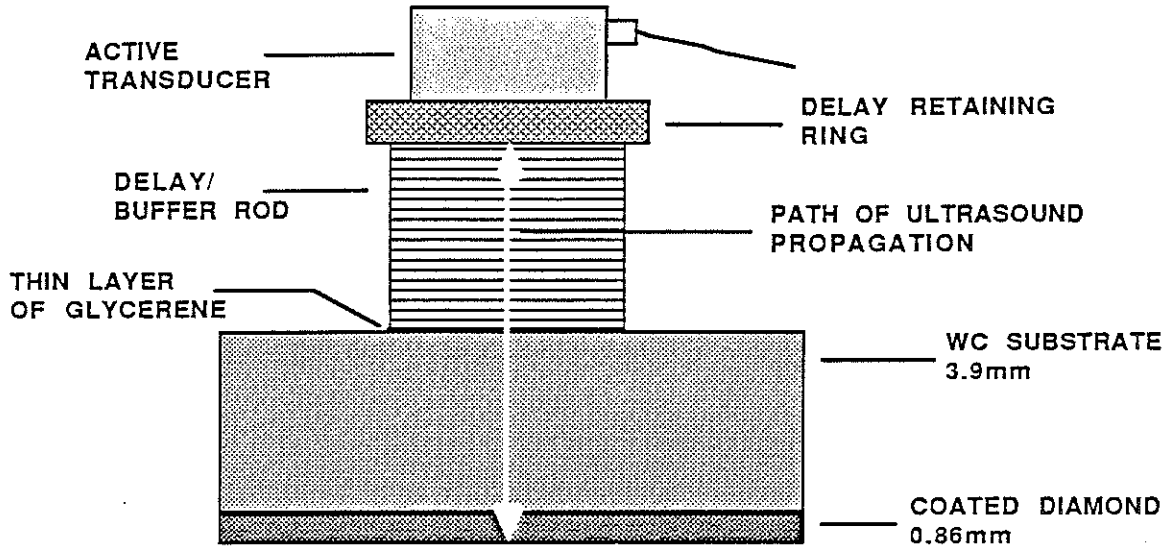

FIG. 16. Coupling of a delay line λ- series transducer to a diamond-deposited WC tool showing the critical dimensions of the test sample.

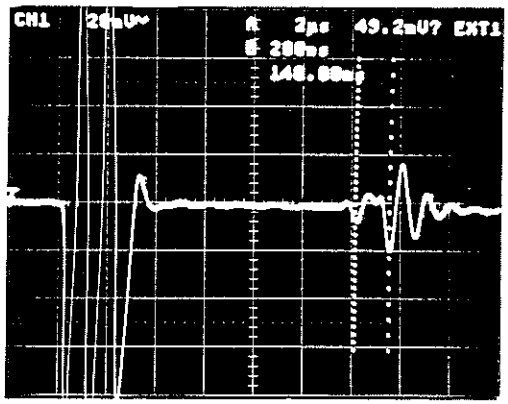

Fig. 17. Ultrasonic observations from the test set up shown in Fig. 16.

Extreme Left: Transducer delay - WC interface.
2nd from Left: WC - diamond interface.
Extreme Right: Diamond - ambient interface.

Measured time-of-flight through diamond (between two cursors): 140ns
Velocity of ultrasound through diamond: 12,285m/s.

Measured time-of-flight through WC: 1.14µs.
Velocity of ultrasound through WC: 6,840m/s

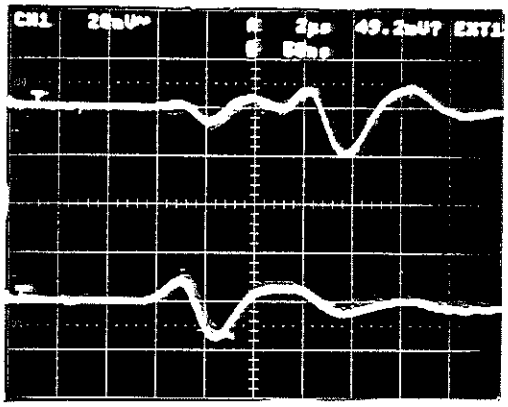

Fig. 18. Characterization of a multi-layer ferrite composite for the quality of bond between Barium Titanate and glass.

Top Trace: Defect-free or "good" bond quality region. Left indication corresponds to Barium Titanate - glass interface, while the right indication is from glass - ambient interface. The time-of-flight between these two indication corresponds to glass thickness, which is only 0.4mm.

Bottom Trace: Defected or partially bonded region. Observe, the amplitude of Barium Titanate - glass interface is higher than one in the top trace, while that of glass - ambient is lower. This indicates partial to total disbond at glass - Barium Titanate interface.

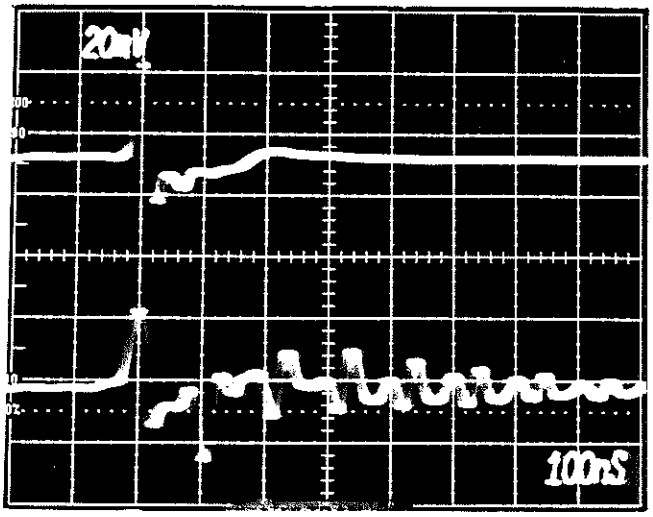

Fig. 19. Simultaneous high resolution and defect detectability by utilizing water immersion method and a 10MHz, 6mm active area diameter and 19mm point focused λ- series transducer. Test sample used for this demonstration is an aircraft quality aluminum with an artificial 1.0mm defect located at 0.4mm from the testing surface.

Top Trace: Indication of water - aluminum interface on an apparently defect-free zone.
Bottom Trace: Indication from the defect at 0.4mm. Observe 100% resolution of this defect with several multiple reflections.

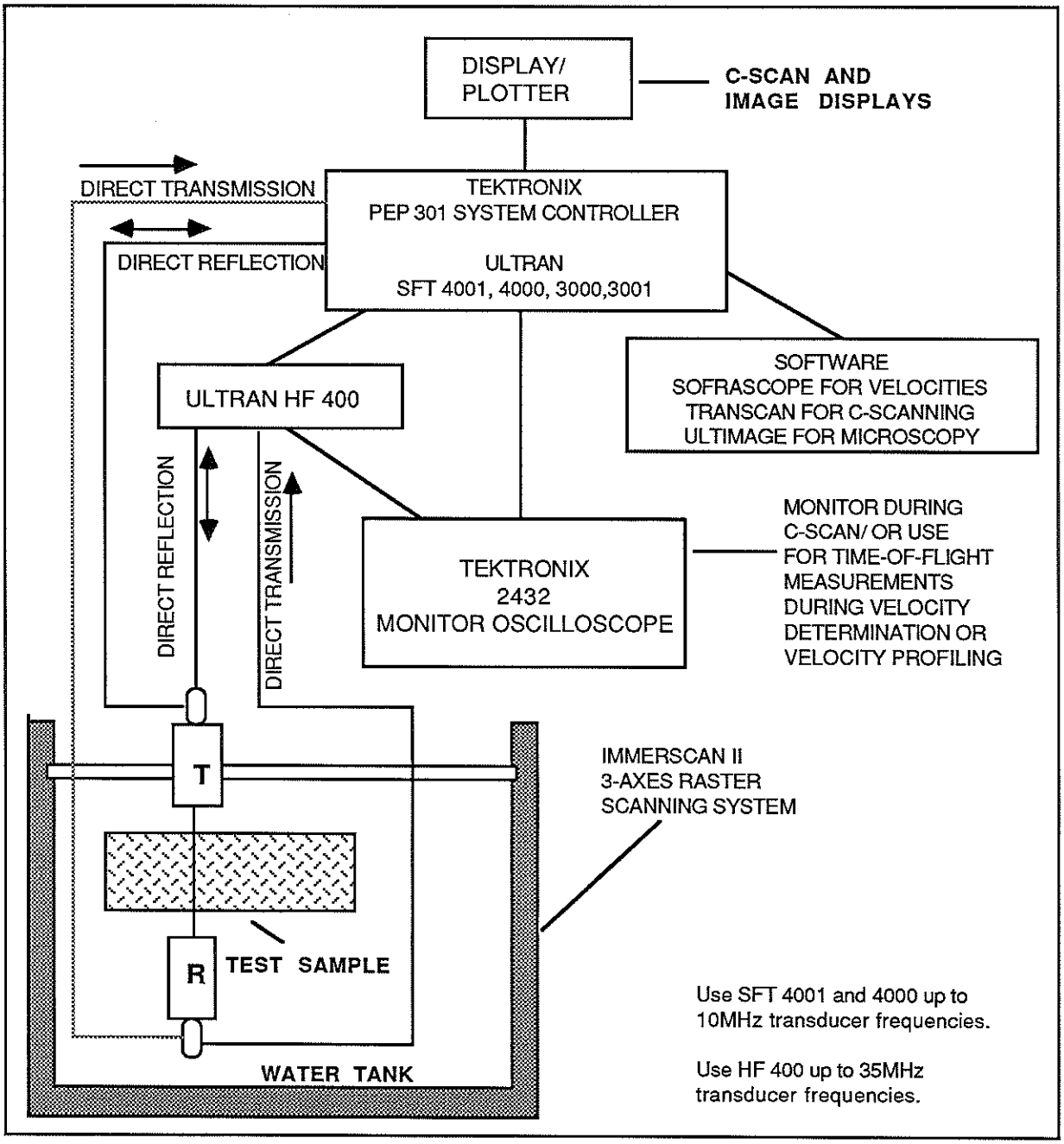

Fig. 20. A schematic layout describing the arrangement of ultrasonic and computer hardware and utilization of software of NDC 7000 system for ultrasonic imaging. This system can also be used to conduct velocity and frequency profilometric studies, as well as for acoustic and field characterization of ultrasonic transducers.

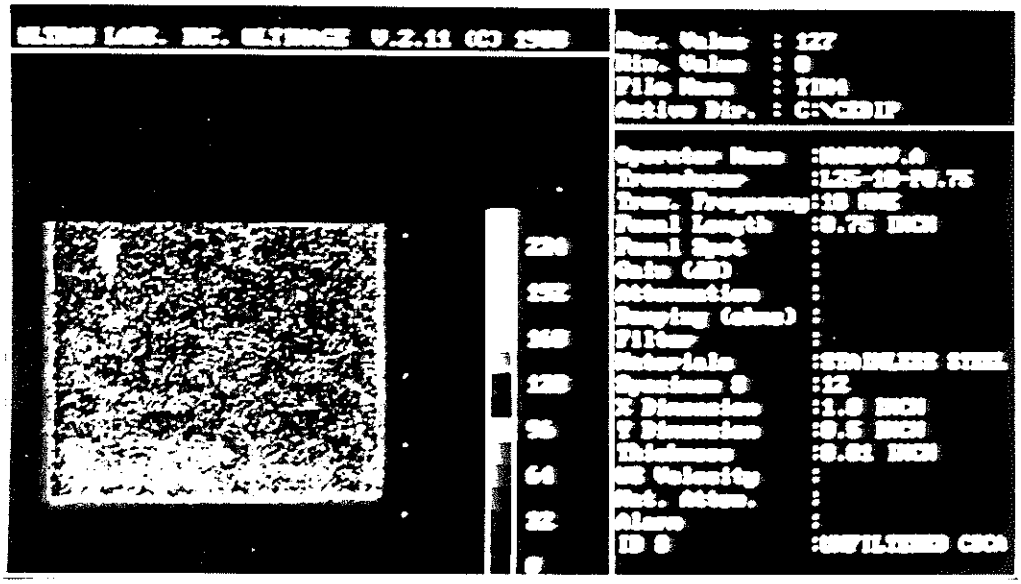

Fig. 21. An unprocessed C-scan of a 1.6mm thick carbon steel indicating "overall" homogeneity of the material. Total area analyzed is: 6x8mm.

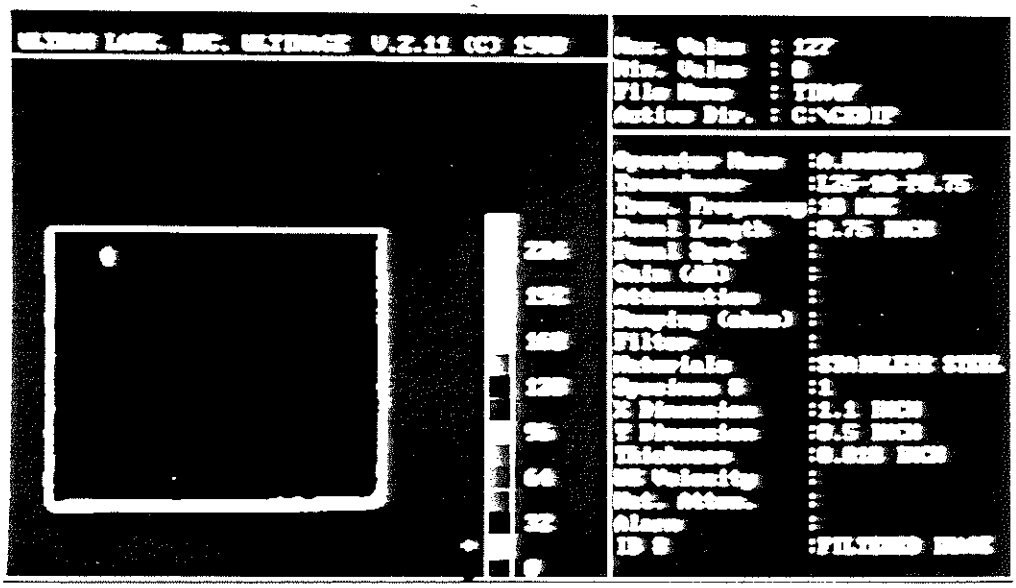

Fig. 22. Same as above, except processed by ULTIMAGE, an image processing software. Observe the detection of an 75μm artificial defect at the upper left hand corner, located at 0.25mm in the steel specimen.
Method: Monitoring of bottom surface reflected signal.
Transducer: λ - series: 6.0mm active area diameter, 10MHz, and 19mm point focus in water.

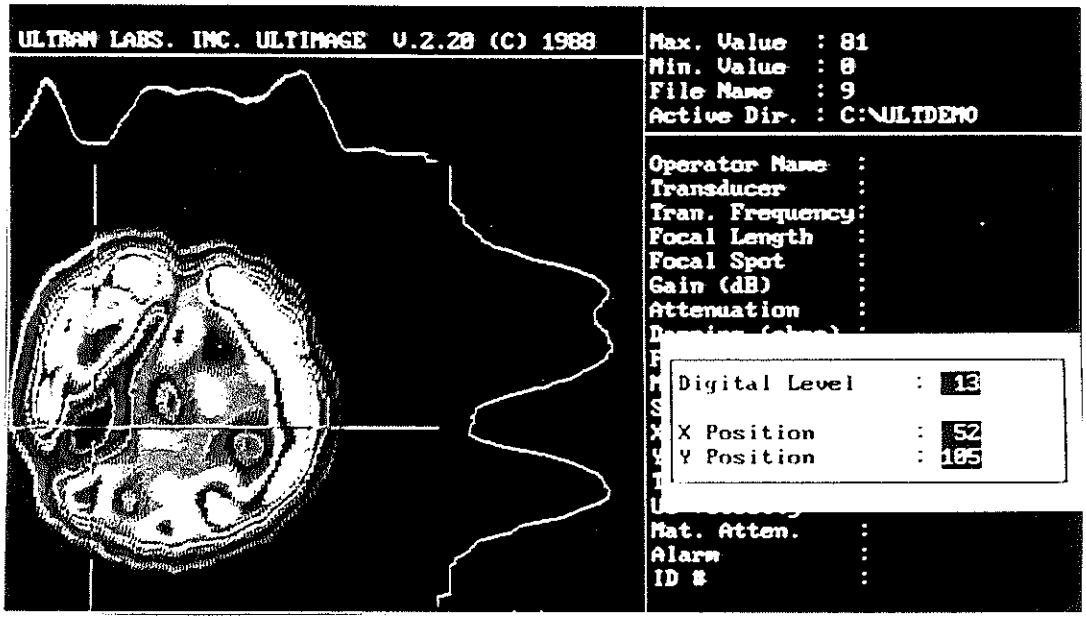

Fig. 23. Internal image and cross-sectional profiles of a crystalline glass - 25mm diameter and 3mm thick. Note, the cursors are intersecting at an apparent pore, also indicated by the digital level of the top and right cross-sectional profiles. Other fluctuations in these profiles may be due to chemical and/or micro-structural characteristics of the sample analyzed.

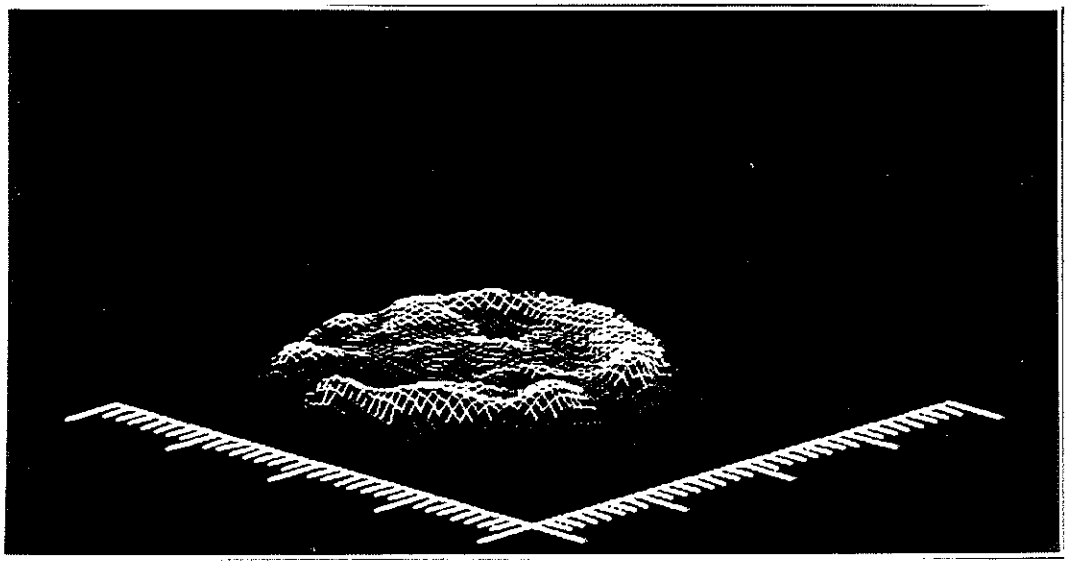

Fig. 24. Same as above, except, a 3-D representation. Compare the similarities of various regions of this point-of-view with those in Fig. 23.
Method: Monitoring of bottom surface reflected signal.
Transducer: λ - series: 6.0mm active area diameter, 10MHz, and 19mm point focus in water.

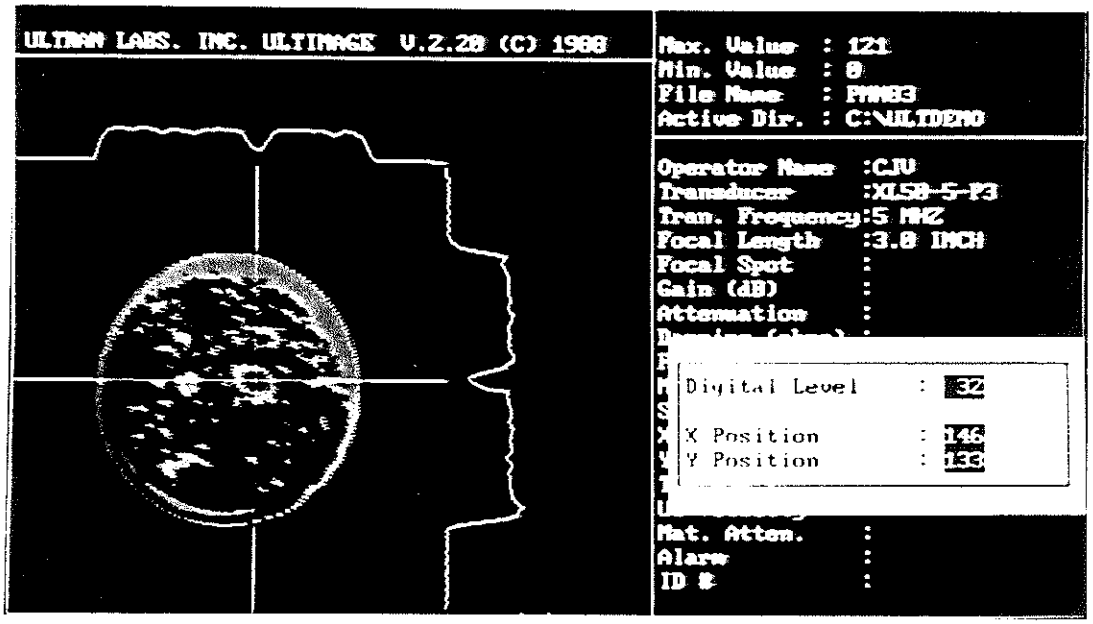

Fig. 25. Internal image and cross-sectional profiles of a commercial Lead Zirconate - Lead Titanate material - 38mm diameter and 4.3mm thick. The cursors are intersecting at an apparent defect, also enhanced by the digital levels of the top and right profiles. Other variations, indicated by color enhancement and in the cross-sectional profiles are believed to be caused by stoichiometric heterogeneity of the sample.
Method: Monitoring of bottom surface reflected signal.
Transducer: λ -series: 13mm active area diemeter, 5MHz, and 76mm point focus in water.

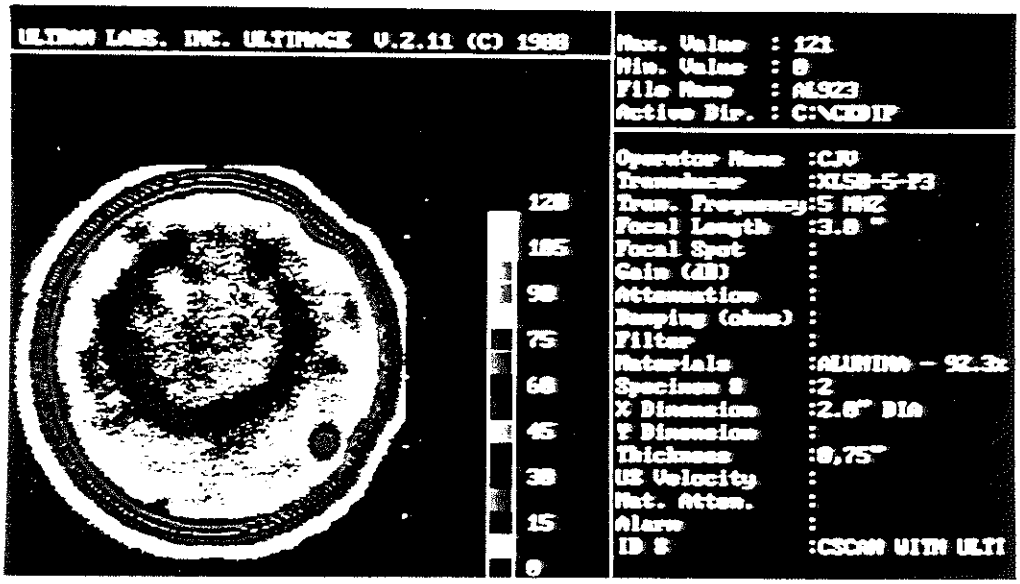

Fig. 26. Enhacned ultrasonic image from a 51mm diameter and 13mm thick specimen of 92.3% sintered alumina, exhibiting subtle density variations, indicated by sharp colored rings. At the lower right hand region is the appearance of an apparent pore. It is interesting to note that an ordinary C-scan failed to reveal the micro-structural details of this specimen.
Method: Monitoring of bottom surface reflected signal.
Transducer: λ - series: 13mm active area diameter, 5MHz, and 76mm point focus in water.

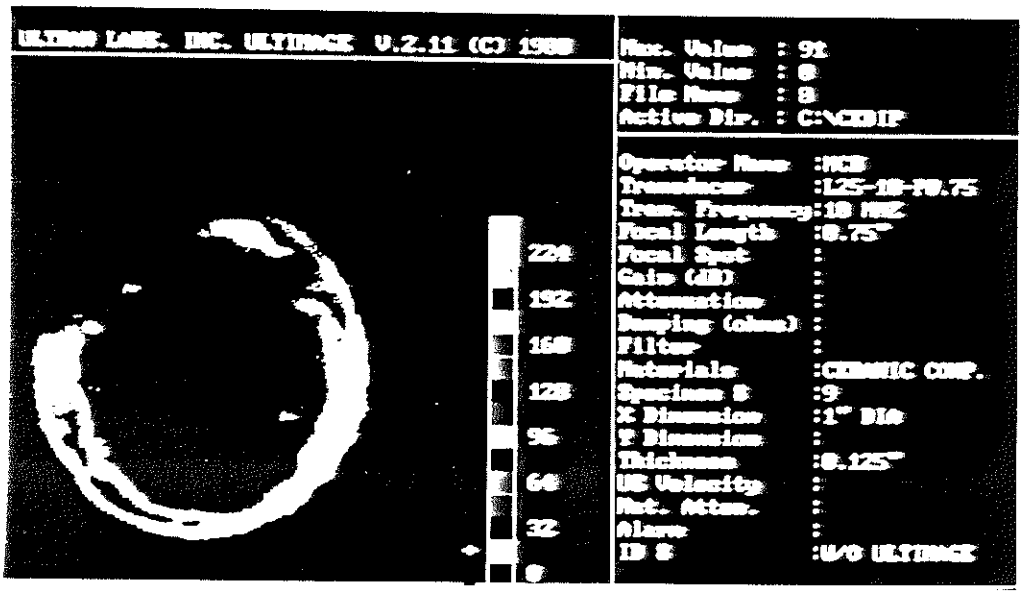

Fig. 27. An ordinary or unprocessed C-scan of a Lithia-Alumina-Silica composite - 25mm diameter and 3mm thick - indicating a large central void and some defective regions in the out ring, through which ultrasound propagated relatively easily.

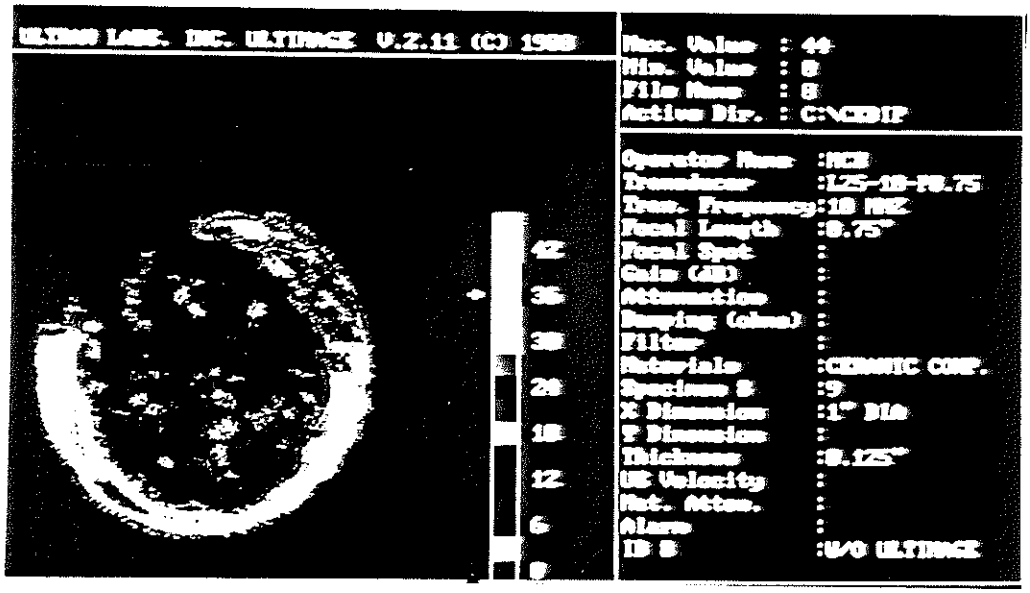

Fig. 28. An ULTIMAGE processed image of Fig. 27, indicating finer micro-structural details of the central and outer regions of the sample analyzed. Bright blue speckles are believed to be caused by scatter from crystalline targets.
Method: Monitoring of bottom surface reflected signal.
Transducer: λ - series: 6.0mm active area diameter, 10MHz, and 19mm point focus in water.

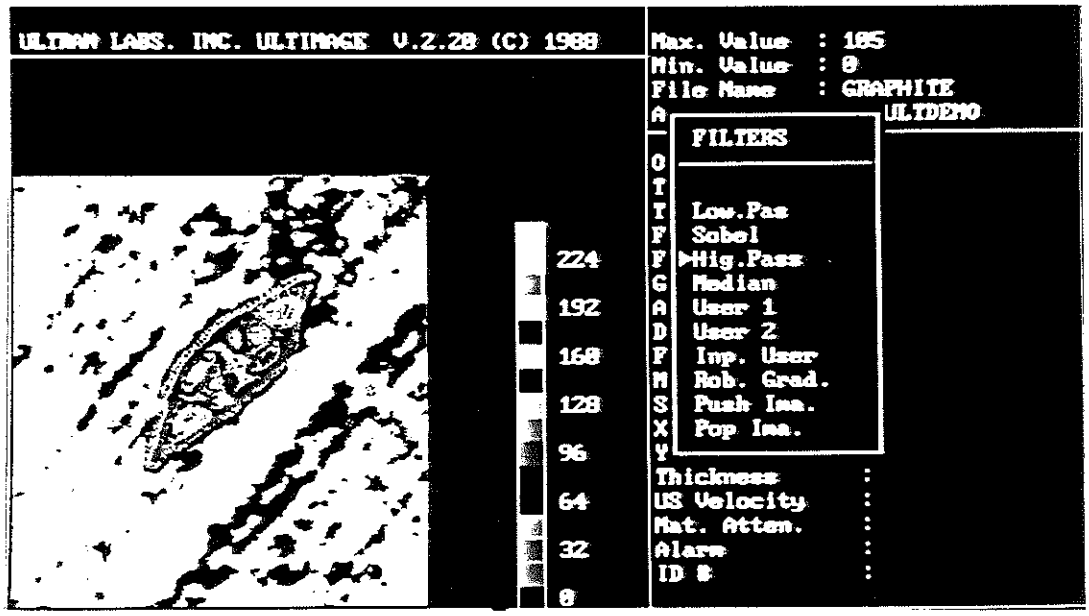

Fig. 29. A high pass-filtered ULTIMAGE representation of impact damage in a Graphite Fiber Reinforced Plastic Composite, 1.4mm thick. Total area examined is 13 x 13mm. Green lines are caused by the scatter of ultrasound by graphite fibers, while the central region describes the complete geometry of impacted region. Observe further details of fiber breakage within the diamond-shaped indentation.
Method: Monitoring of bottom surface reflected signal.
Transducer:λ -series: 6mm active area diameter, 5MHz, and 25mm point focus in water.

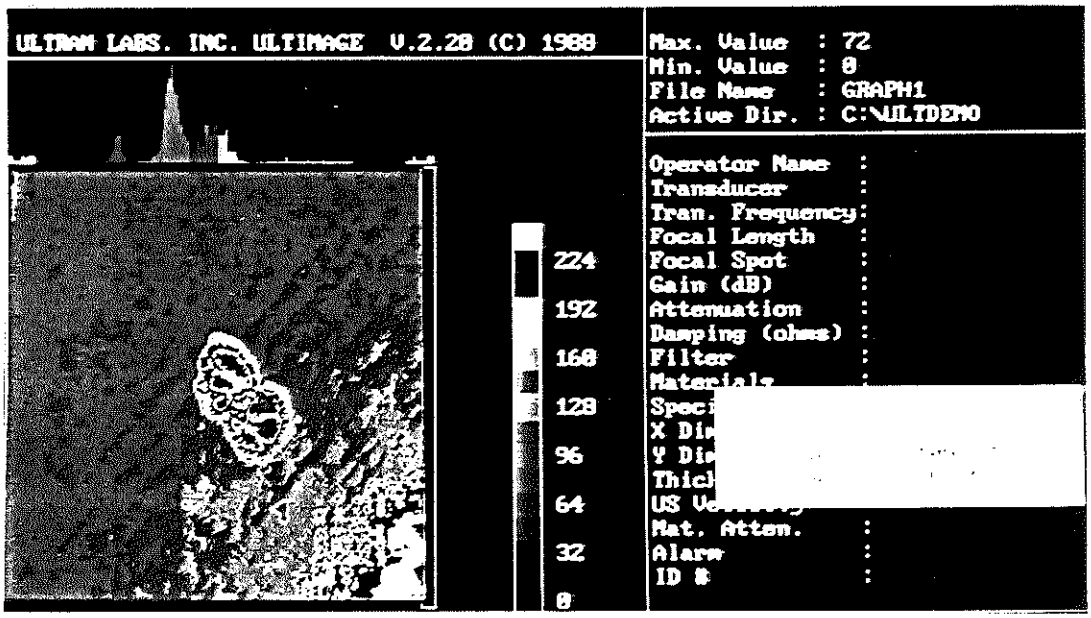

Fig. 30. An internal image of the composite specimen analyzed in Fig. 29 by monitoring the scattering of ultrasound from within the sample. This describes further details of the impacted region as it appears within the sample thickness. Also, observe more internal fiber damage and delaminations at the lower right hand corner. The top portion of the figure shows a digital histogram indicating the relative damage as a function of scatter signal strength.
Method: Monitoring of internal ultrasound scatter.
Transducer:λ - series: 6.0mm active area diameter, 10MHz, and 19mm point focus in water.

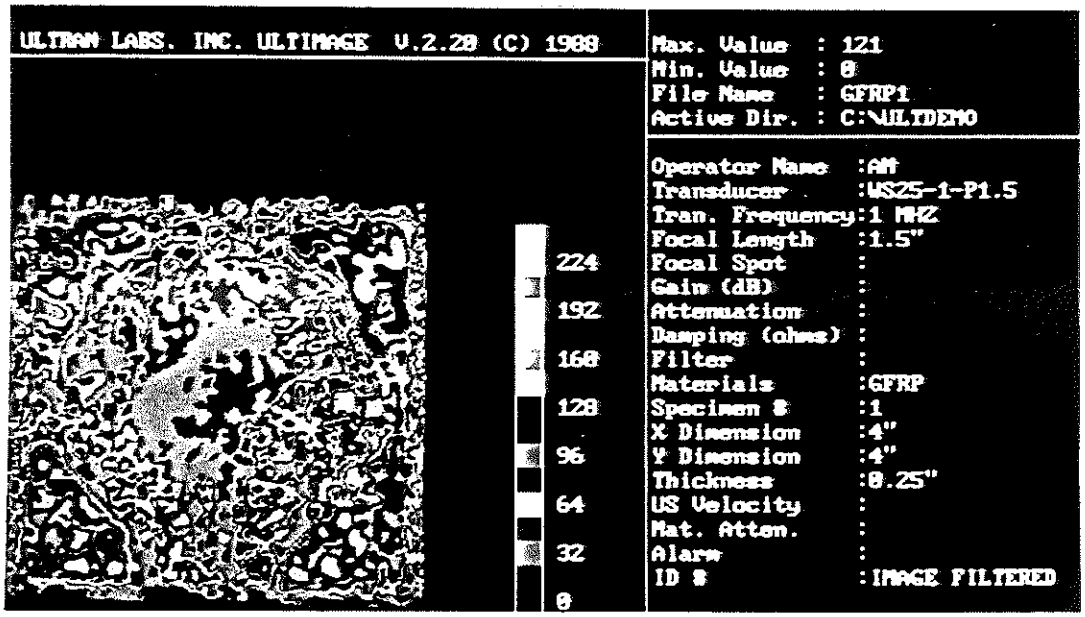

Fig. 31. An ultrasonic image of a Glass Fiber Reinforced Plastic Composite - 100 x 100mm area and 6mm thick - sample. This sample was catastrophically damaged by a 76mm diameter target, indicated by the central circular region. Observe the indications of relatively undamaged regions, enhanced at the four corners of the sample.
Method: Monitoring of bottom surface reflected signal.
Transducer used: λ -series 25mm active area diameter and 100mm point focus in water.

A Pre-print of a Paper on "IMPORTANT CONSIDERATIONS AND EXPERIMENTAL PROCEDURES FOR PROPERTIES MEASUREMENT AND INTERNAL IMAGING BY MODERN ULTRASONIC METHODS," by Mahesh C. Bhardwaj.

Submitted to the Ceramic Bulletin, the American Ceramic Society - October 1988

redefining
the limits of
ultrasound

ultran laboratories, inc.
139R north gill street
state college, pa 16801 usa
814.238.9083 *phone*
82.0978 *telex*
814.234.3367 *fax*